ÉCOLE CENTRALE DE NANTES 2016-2017

EMARO+ M1
European Master on Advanced Robotics

Platoon Modelling and Control

Project Report

Presented by

Aman SHARMA and Prajval Kumar MURALI

On 27th June 2017

Jury

Evaluators:	Matthew STEIN	Professor (RWU)
	Gaëtan GARCIA	Professor (ECN)
Supervisor(s):	Philippe MARTINET	Professor (ECN)

Abstract

Control of a platoon is of great interest to researchers and engineers who envisage to develop robust solutions to increase the traffic density while adhering to stringent safety standards and maintaining comfort. The presented work focuses on development of a methodology to generate an offline trajectory to be followed by a platoon of vehicles from a given set of points. The aim is to generate a highly smooth trajectory so as to ensure a minimum continuity in curvature. Apart from generation of a plausible smooth trajectory, necessary methodology is also proposed to numerically compute the pose of each vehicle in Frènet frame. The proposed methodology enables straight-forward implementation of linearized decoupled control laws to manipulate the longitudinal speed and steering angle of each vehicle to accomplish successful platooning. To achieve the aforementioned objectives, firstly kinematics model of a vehicle would be presented in Frènet space to obtain the dynamically evolving system. After obtaining the model in Frènet basis, a linearized decoupled control law will be used to manipulate longitudinal speed and steering angle. It will be later shown that in-order to exactly decouple and linearize the system, it is necessary to exactly parametrize the trajectory in terms of curvilinear distance and be able to compute the curvilinear abscissa of nearest point of the trajectory from vehicle and be able to measure the curvature and it's derivative at this point. A methodology will be proposed, by utilizing already existing mathematical tools, to numerically compute all the desired parameters necessary for controlling a platoon. The robustness of the controllers will be tested with proportional-derivative controller and sliding mode controller. The validity of proposed methodology is tested by means of simulation study for local, global and hybrid platoon control architecture to make concluding remarks and necessary inferences.

Acknowledgements

We would like to thank our supervisor Prof. Philippe MARTINET for his constant support, guidance and encouragement throughout the work. His experience and wisdom, as a vibrant researcher, helped us to resolve several juggernauts in devising various methodologies proposed and implemented in the report. Moreover he addressed all our questions, comments and difficulties with a smile and ascertained us with several technical nuances from time to time. We also thank him for his time to expose us to the state of art autonomous vehicles present at LS2N and introducing us to research engineers working in the Laboratory.

We would like to extend our thanks to Prof. Gaëtan GARCIA for administratively managing the project.

Contents

Chapter 1

Introduction

A group of vehicles that can travel together closely, safely and at high speed is referred to as a platoon. Vehicle platooning is a strategy which is envisaged to be imbibed in next-generation vehicles to meet future demands and achieve higher degree of autonomous behaviour. Generally speaking, for a platoon, there exists a lead vehicle which decides the trajectory to be followed by the subsequent vehicles. The vehicles communicate with the main leader and also their immediate neighbour just in front from them. For platooning to be successful, all the following vehicles (which have precisely matched braking and acceleration) must respond in accordance to the lead vehicle's movement. The vehicles used for platooning are made autonomous so as to ensure that they can be driven by an on-board computer. Safety is of utmost importance while platooning and hence it is necessary to have robust control topology which is fault tolerant.

1.1 Problem Formulation

Controlling of a Platoon is an extremely diverse problem by itself and therefore it is absolutely pertinent to describe the scope of project clearly. The back-ground of subject under investigation goes as follows: A *real-life* leader is made to follow an offline trajectory. The goal is to use an appropriate vehicle kinematic model and control the desired state variables of the model in-order to drive the platoon along this known trajectory.

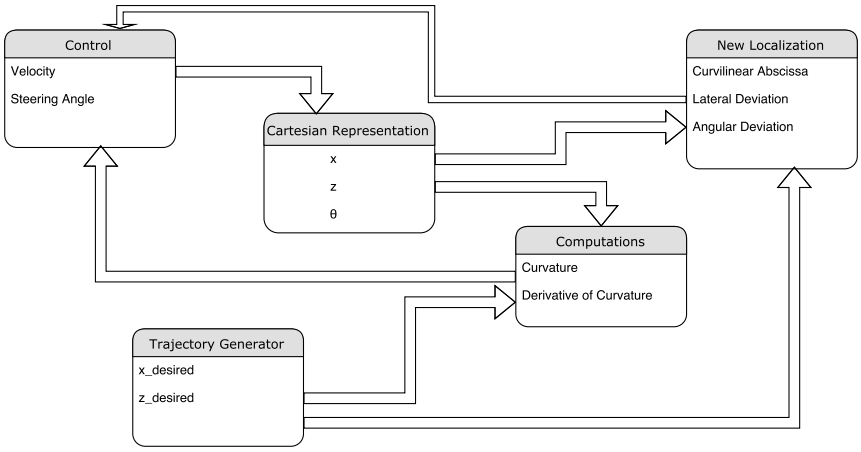

Figure 1.1: Top View of the subject under investigation

A schematic view of the problem statement is portrayed by means of a flow chart depicted in fig. 1.1. This flow chart shall serve as the basis of all subsequent discussions and organization of work. The block named *New Localization* uses the data associated with desired trajectory and current Cartesian localization to yield a new localization system. The control law is based on the kinematics associated with new localization parameters and certain characteristics of desired trajectory. Control signal is comprised of two entities namely longitudinal speed and steering

angle. It will be later presented that both longitudinal speed and steering angle control laws are decoupled and this allows division of control problem into design of two separate controllers: lateral control and longitudinal control. All of these blocks will be presented in subsequent chapters.

1.2 Organization of Report

Based on the problem requirements, following arrangement seems suitable to ensure smooth comprehension of illustrations and concepts utilized, developed and marginally researched in the report:

- Chapter 2 is dedicated to presenting the existing state of art that have been developed by researchers in the domain of Platooning.
- Chapter 3 is dedicated to demonstration of vehicle kinematics using non-conventional parameters which include curvilinear abscissa, lateral deviation and angular deviation in-spite of standard three degree of freedom representation comprising of Cartesian co-ordinates and orientation. The reason for using this representation will also be briefly discussed in the concerned chapter.
- Chapter 4 is dedicated to finding an appropriate control law so as to manipulate the longitudinal speed and steering angle of an individual vehicle to facilitate platooning. The system model is highly non-linear and in-order to employ a linearly decoupled control, the system model is transformed as a chained system with it's dynamics varying solely with respect to distance and not time. This will be explicitly detailed in the concerned chapter
- Chapter 5 is dedicated to generation of trajectory and calculation of certain geometric parameters associated with the trajectory.

  .

Chapter 2

Literature Survey

Automation of vehicles is burgeoning due to the following: traffic density, efficiency, safety and comfort. The present century has witnessed some intelligent vehicles and ITS solutions which include Google Car, VIP, and car manufacturers have already developed certain solutions (Tesla, Audi, Mercedes, Renault, PSA, Nissan, Fiat...). Efforts are currently being made by researchers and industry to enhance performance, reliability and reducing the cost.

Usually lateral and longitudinal dynamics of a vehicle are coupled. Associated dynamics can be decoupled in a pretty much straightforward fashion when using a kinematic vehicle model [1], however for high velocity applications, a kinematic model cannot be put to use. Controllers are assumed to be decoupled for low curvature paths such as highways thereby allowing independent design of longitudinal and lateral control laws [2]. The work presented in [3] demonstrates an implementation of lateral control assuming it to be sufficiently independent from longitudinal control. Whereas in [4], lateral and longitudinal controllers were designed independently: parameters of lateral controller were calculated for different set of speeds and saved in a look-up table. However at high speeds and/or on tightly curved roads, coupling between the two dynamics cannot be ignored.

The primary objective of lateral control is to force the vehicle to follow a desired path by settling the lateral and angular deviations to zero. Many control strategies have been used in the past to accomplish lateral control: either based on accurate kinematic or dynamic vehicle model (e.g. H∞ [5]) or rough vehicle models (e.g. sliding mode [6], [7] or adaptive control algorithms [8], [9]). On the other hand there exists certain strategies which do not make use of any vehicle model (pure pursuit [10], Stanley [10], fuzzy logic [11]). The work presented in [9] underscores an adaptive PID controller on a real automated vehicle. The nominal kinematic model of vehicle was extended in [12] to accommodate two sliding parameters under consideration, the estimation of these two parameters is incumbent on an observer.

Vehicular congestion is an evident problem in urban areas which leads to loss of time. Automated platooning could be one of the solutions to tackle this problem. Concretely speaking, several autonomous vehicles could be made to follow the trajectory of a leader, with predefined safe inter-distance among themselves. Different platooning approaches have been proposed in the past. These approaches may be broadly classified into three major categories, based on the information used for vehicle control, as follows: local, semi-global and global strategies. The most common and classical approaches invoke local control strategy, i.e. each vehicle communicates exclusively with the immediate leader. This approach is also known as leader-follower approach. Visual tracking of the immediate preceding vehicle was proposed in [13] and generic control strategies have been proposed in the past as discussed in [14] and [15]. Certain strategies which enforce formation keeping utilize semi-global strategies: that is a vehicle communicates

with neighboring vehicles (not only the preceding one). The aforementioned approaches are convoyed with certain limitations, firstly error accumulation: the servoing errors, induced by sensor noises and/or actuator delays inevitably grow while being propagated from the leader to subsequent vehicles, leading to unacceptable oscillations. Global strategy is a way out of this conundrum, which is based on communication of a vehicle with all the vehicles. In [16], a mechanical analogy was used in designing a feedback based control to achieve straight line motion. A single virtual rigid structure inspired by graph theory was considered in [17].

Trajectory generation mechanics, pertinent to the domain of robotics, have been extensively discussed in [18], [19], [20]. However for platooning applications, a high-order continuity in the trajectories (at least C2) is quintessential. Several approaches derived from Computer Aided Design community appear attractive: the work demonstrated in [21], [22], [23] uses parametric functions like Bézier curves and B-Splines to fit smooth trajectory according to boundary conditions. Curvature based constraints were investigated in [24]. Trajectory modification in dynamic environment and on-line navigation techniques were investigated in [25], [26], [27].

A few photographs of several research projects that have been successfully implemented in the past are shown below as a part of literature survey.

(a) Project Autolib

(b) Project Konvoi

(c) Project Mobivip

(d) Project Path

Chapter 3

System Modelling

The primary goal of this chapter is to motivate a transformation of three degree of freedom Cartesian representation of a vehicle to Frènet frame. Later, the variables of this frame will be used to design a control law to accomplish successful platooning. A car-like mobile robot (rear-drive) is composed of a motorized wheeled axle at the rear of the chassis, and one (or a pair of) orientable front steering wheel(s) as shown in fig 3.1.

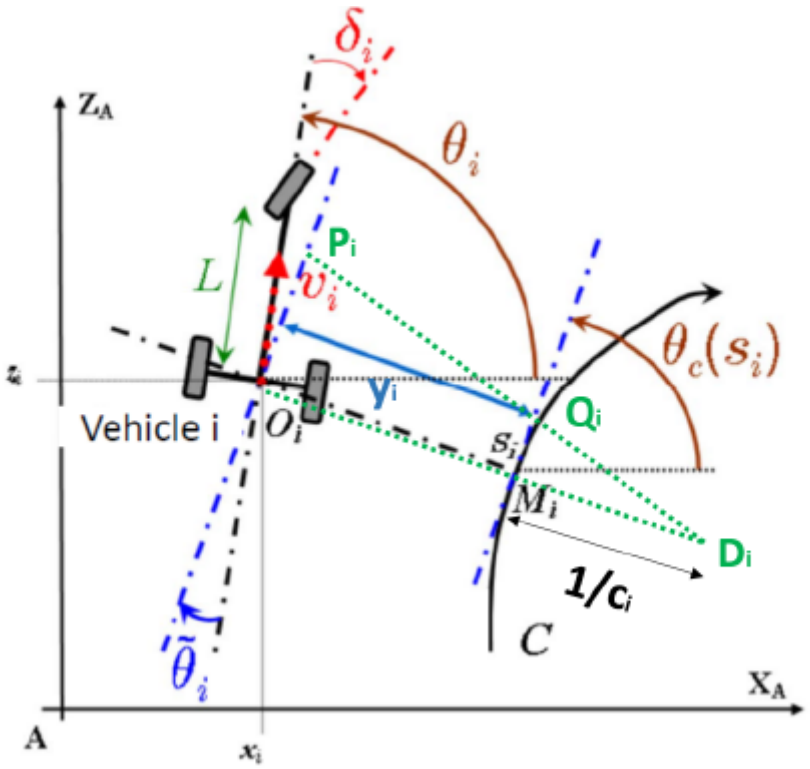

Figure 3.1: Bicycle Model [1,1] Robot

3.1 Notation

Throughout the report we shall adhere to the following notations and one can consider it to be uniform unless otherwise explicitly mentioned.

- C : Reference/desired Path
- s : Curvilinear abscissa
- s_0: Initial curvilinear abscissa

- $c(s)$: Local curvature
- $1/c(s)$: Radius of curvature
- θ_i : Orientation of the vehicle i with respect to world frame
- $\theta_c(s_i)$: Orientation of the tangent to the trajectory at the same point in relation to the Absolute reference
- $\tilde{\theta_i}$: Angular deviation of the vehicle i from the trajectory C
- δ_i : Steering angle of vehicle i
- v_i : Longitudinal Velocity of vehicle i
- y_i : Lateral deviation off vehicle i from C
- L : Wheelbase of the vehicle
- O_i : Origin of frame for vehicle i.

3.2 Kinematic Modelling

The control inputs U to the system represented above are:

- Longitudinal Velocity, v
- Steering Angle, δ

The state variables are:

- Curvilinear Abscissa s
- Lateral deviation, y
- Angular deviation, $\tilde{\theta}$

Following the general direct kinematic model for [1,1] type robots, we have:

$$\dot{x_i} = v_i \cdot \cos\theta_i$$
$$\dot{z_i} = v_i \cdot \sin\theta_i$$
$$\dot{\theta_i} = \frac{v_i}{L} \cdot \tan\delta_i$$

Given that Cartesian distance is not monotonous for very curved trajectories while quantifying the spacing between two consecutive vehicles, it is necessary to re-express the model in curvilinear space, that is, with respect to the curvilinear abscissa of the nearest point on the trajectory measured from the vehicle, as seen in figure 3.2. Thus modelling in a **Frénet frame**:

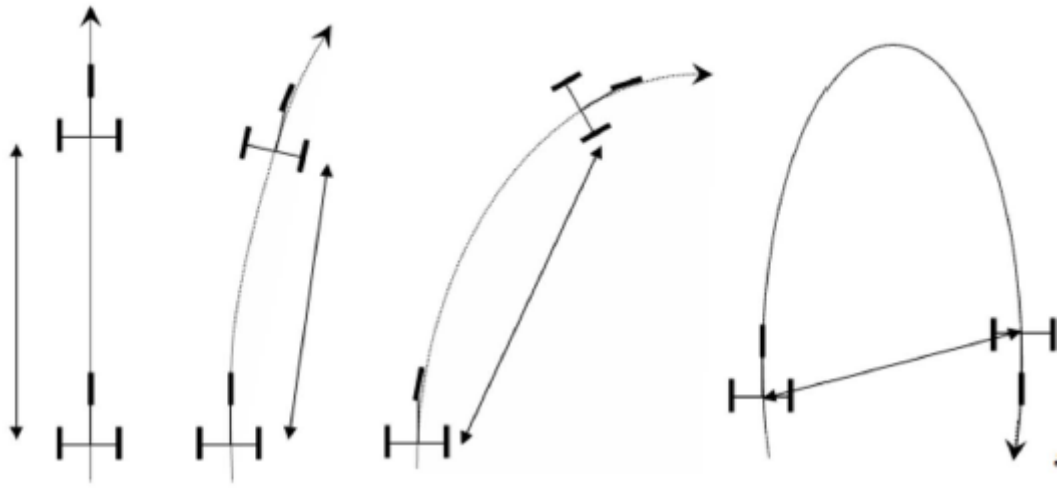

Figure 3.2: Curvilinear distance vs Cartesian distance

O_iP_i represents the projection of the Cartesian velocity of the vehicle into rotated space and $\dot{s}_i$ $= M_iQ_i$ the further projection by considering the lateral deviation y_i . The symbol c_i stands for the respective local curvature, which corresponds to the reciprocal of the radius of curvature.

$$\frac{D_iM_i}{D_iO_i} = \frac{M_iQ_i}{O_iP_i}$$

$$\frac{1/c_i}{1/c_i - y_i} = \frac{\dot{s}_i}{v_i cos\tilde{\theta}_i}$$

$$\dot{s}_i = \frac{v_i cos\tilde{\theta}_i}{1 - y_i c_i}$$

$$\dot{y} = v_i sin\tilde{\theta}_i$$

But we know that $r_{c_i} \cdot \theta_c = s$ where $r_{c_i} = 1/c_i$ we can get:

$$\theta_c = s \cdot c_i$$
$$\dot{\theta}_c = \dot{s} \cdot c_i$$

Given that $\tilde{\theta}_i = \theta_i - \theta_c$ we get the system equations as follows:

$$\dot{s}_i = \frac{v_i \cdot cos\tilde{\theta}_i}{1 - y_i c_i} \tag{3.1}$$

$$\dot{y}_i = v_i \cdot sin\tilde{\theta}_i \tag{3.2}$$

$$\dot{\tilde{\theta}}_i = v_i \left(\frac{tan\delta_i}{L} - \frac{c_i \cdot cos\tilde{\theta}_i}{1 - c_i y_i} \right) \tag{3.3}$$

Chapter 4

Control Strategy

Control of a convoy is comprised of two independent controls viz. longitudinal control and lateral control. Longitudinal control ensures following of the leader by keeping a desired distance between the vehicles. The main goal of longitudinal control is to allow small distance between the vehicles while ensuring the stability and safety of the convoy. The role of lateral control is to minimize the lateral distance of the convoy from desired trajectory. Longitudinal and lateral control of vehicles are totally uncoupled and hence they can be computed separately. This chapter addresses the control strategies used for a convoy of autonomous vehicles in an urban environment.

4.1 Platoon control objectives

- Maintain the inter-vehicle distance
- All vehicles must move at the same speed
- Trajectory tracking
- Stable platoon based on string stability
- Increased traffic density
- Safety (no collision)
- Urban/ Highway platooning
- Homogeneous and non-homogeneous platoon
- Stability and safety during total communication loss and in presence of time delay (actuator delay/communication delay).

4.2 Lateral Control

In this section two different controllers are designed for implementing the lateral control: Proportional-Derivative (PD) controller and Sliding mode controller. Choice of path tracker influences the performance in terms of precision, stability and passenger comfort. In choosing a lateral controller, simplicity, efficiency and robustness are considered as the main criteria.

4.2.1 PD Controller

Consider a general chain form system:

$$\dot{a_1} = m_1$$

$$\dot{a_2} = a_3 m_1$$

$$\dot{a_3} = a_4 m_1$$

$$\dots \dots$$

$$\dot{a_{n-1}} = a_n m_1$$

$$\dot{a_n} = m_2$$

Consider the transformation for an Order 3 chain system as:

$$a_1 = s \implies m_1 \triangleq \dot{a_1} = \frac{vcos\tilde{\theta}}{1-cy}$$
$$a_2 = y \implies a_3 m_1 \triangleq \dot{a_2} = vsin\tilde{\theta}$$
$$a_3 = tan\tilde{\theta}1 - cy$$
$$m_2 \triangleq \dot{a_3} = -c.v.sin\tilde{\theta}tan\tilde{\theta} - g\frac{vcos\tilde{\theta}}{1-cy}tan\tilde{\theta}y + \frac{(1-cy)v}{cos^2\tilde{\theta}}\left(\frac{tan\delta}{L} - C\frac{cos\tilde{\theta}}{1-cy}\right)$$

where $\frac{d}{dt}(c(s)) = g \cdot \dot{s}$

Hence State Mapping: $\mathbf{A} = \Theta(\mathbf{X})$
Control Mapping: $\mathbf{M} = \Upsilon(\mathbf{U}, \mathbf{X})$
where $\mathbf{U} = (v, \delta)$ and $\mathbf{X} = (s, y, \tilde{\theta})$ and

$\Theta(\mathbf{X}) = (s, y, (1-cy)tan\tilde{\theta})$
$\mathbf{M} = \left(\frac{vcos\tilde{\theta}}{1-cy}, -c.v.sin\tilde{\theta}tan\tilde{\theta} - g\frac{vcos\tilde{\theta}}{1-cy}tan\tilde{\theta}y + \frac{(1-cy)v}{cos^2\tilde{\theta}}\left(\frac{tan\delta}{L} - C\frac{cos\tilde{\theta}}{1-cy}\right)\right)$.

It is possible then to replace $\frac{d()}{dt}$ by $\frac{d()}{da_1}$ to reach the next expression:

$$a_1' = 1$$
$$a_2' = a_3$$
$$a_3' = m_3$$

with $m_3 = \frac{m_2}{m_1}$. Notice that from here it is straight forward to propose a control law that ensures convergence on a_2 and a_2'. One proposes thence exponential convergence of the form:

$$m_3 = -K_d \cdot a_3 - K_p \cdot a_2$$

such that

$$a_2'' + K_d \cdot a_2' + k_p \cdot a_2 = 0$$

corresponding to $y \to 0$ and $tan\tilde{\theta} \to 0$ for $\tilde{\theta} \neq \frac{\pi}{2}$ and $v \neq 0$

Thus ensuring convergence in the lateral deviation and the angular deviation iff K_p and K_d conform to a Hurwitz polynomial of order two. Given that m_2 and m_1 were already defined, m_3 can be formed out of their definitions as shown here:

$$m_3 = -c.tan^2\tilde{\theta}(1-cy) - g.y.tan\tilde{\theta} + \frac{(1-cy)^2}{cos^3\tilde{\theta}}\left(\frac{tan\delta}{L} - \frac{c.cos\tilde{\theta}}{1-cy}\right)$$

From the above equation, one can conclude:

$$\delta(y, \tilde{\theta}) = arctan\left(L\left[\frac{cos^3\tilde{\theta}}{(1-c.y)^2}\left(g.y.tan\tilde{\theta} - K_d(1-c.y)tan\tilde{\theta} - K_p.y + c(1-c.y)tan^2\tilde{\theta}\right) + \frac{c.cos\tilde{\theta}}{1-c.y}\right]\right) \tag{4.1}$$

4.2.2 Sliding Mode Controller

Sliding mode control law is a simple and robust control law which does not require a precise model of the system and can also ensure stability even if the parameters of the system change slowly over time [28].

Assuming the system to be as:

$$\dot{x} = f(x) + g(x) \cdot u$$

$$y = h(x)$$

Sliding mode control strategy is based on Lyapunov stability condition. A function $V(x)$ (representing the energy of the system) is called a Lyapunov candidate function if it satisfies the following conditions:

$$V(x) > 0 \text{ iff } x \neq 0 \tag{4.2}$$

$$V(x) = 0 \text{ iff } x = 0 \tag{4.3}$$

$$\dot{V}(x) \leq 0 \text{ iff } x \neq 0 \tag{4.4}$$

Let us consider the Lyapunov function of the form:

$$V(x) = \frac{1}{2}\sigma(x)^2$$
$$\implies \dot{V}(x) = \sigma(x)\dot{\sigma}(x) \leq 0$$

From the definition we get,

$$\dot{\sigma}(x) = \frac{\partial \sigma}{\partial t} + \frac{\partial \sigma}{\partial x}(f(x) + g(x)u)$$
$$= S_1(x,t) + S_2(x)u$$

Taking $u = u_{eq} + v_n$, where

$$u_{eq} = \frac{S_1(x)}{S_2(x)} \text{ and } v_n = \frac{u_n}{S_2(x)}$$

To satisfy the laypunov condition we can choose

$$u_n = -Ksign(\sigma) \text{ or } u_n = -K\sigma$$

with $K > 0$. The main disadvantage of the former is chattering which can be reduced by using higher-order sliding mode controllers or adaptive sliding mode controller. To ensure stability without chattering, it is sufficient to choose the latter.

Hence the sliding mode control law is:

$$\dot{\sigma} = -K \cdot \sigma \tag{4.5}$$

The sliding surface can be defined as:

$$\sigma = \dot{\tilde{\theta}} + K_\theta \cdot \tilde{\theta} + K_y \cdot y \tag{4.6}$$

where K_θ and K_y are the weighting coefficients.

Equation (3.3) can be linearised by exact linearisation technique using an auxiliary input W_1 to get:

$$\delta = arctan\left(L\left[\frac{W_1}{v} + \frac{c.cos\tilde{\theta}}{1 - c.y}\right]\right) \tag{4.7}$$

This gives:

$$W_1 = \dot{\tilde{\theta}}$$

Using equation (4.5),(4.6), (4.7) we can define the auxiliary input [28] as:

$$W_1 = -\frac{(K + K_\theta)\dot{\tilde{\theta}} + K.K_\theta.\tilde{\theta} + K.K_y.y + K_y.\dot{y}}{K_\theta} \tag{4.8}$$

Equation (4.8) can be plugged into (4.7) to get the required Lateral control law. Note: We must ensure always $v \neq 0$ as this is a singular condition and hence set a lower bound on v.

4.3 Longitudinal Control

The control can be local or global or a combination of the two strategies. The local strategy shown in fig. 4.1 uses the data present on the vehicles, each vehicle is totally autonomous and does not require the use of sophisticated sensors on-board. It can be used in all environments but tracking and inter-distance compliance performance is not very satisfactory.

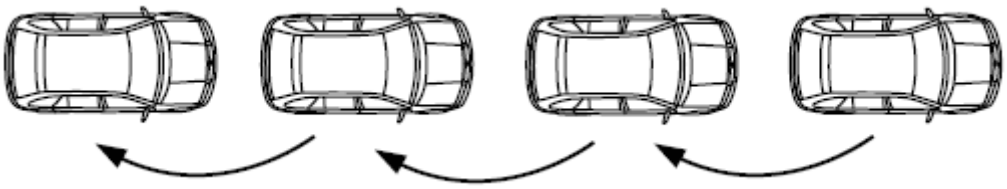

Figure 4.1: Local control strategy [29]

On the other hand, global control strategy as shown in fig. 4.2 uses the data coming from atleast one leader. It requires more sophisticated sensors and reliable communication systems.

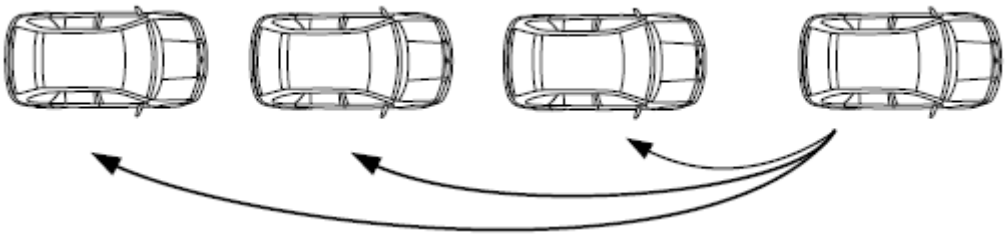

Figure 4.2: Global control strategy [29]

In addition, global control strategy can be centralized or decentralized. In the Centralized control as shown in fig. 4.3, vehicles get their control commands from central units. They are therefore not autonomous and communication is fundamental: any loss or delay in communication is critical. While in a decentralized control as shown in fig. 4.4, each vehicle receives data from other vehicles, but calculates its own control in a stand-alone manner, so that communication remains very important, but that its loss is not as critical as the centralized case [29].

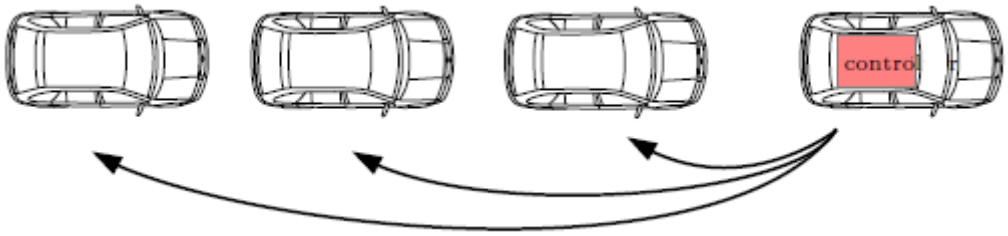

Figure 4.3: Centralized control strategy [29]

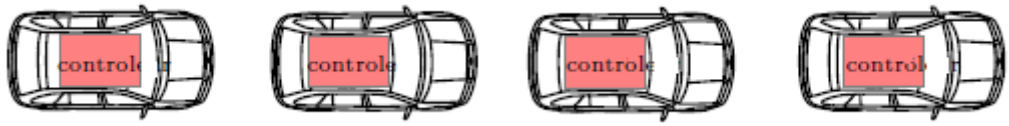

Figure 4.4: Decentralized control strategy [29]

4.3.1 Local Control Strategy

Consider two vehicles as shown in figure 4.5. They are evolving in a plane (x, z), their posture is given by $\eta_i = [x_i, z_i, \theta_i]^T$ for $i = (0, 1)$ and state $\mathbf{X} = (y_i, \tilde{\theta}_i, s_i)^T$. Notice that C is the desired trajectory to be followed.

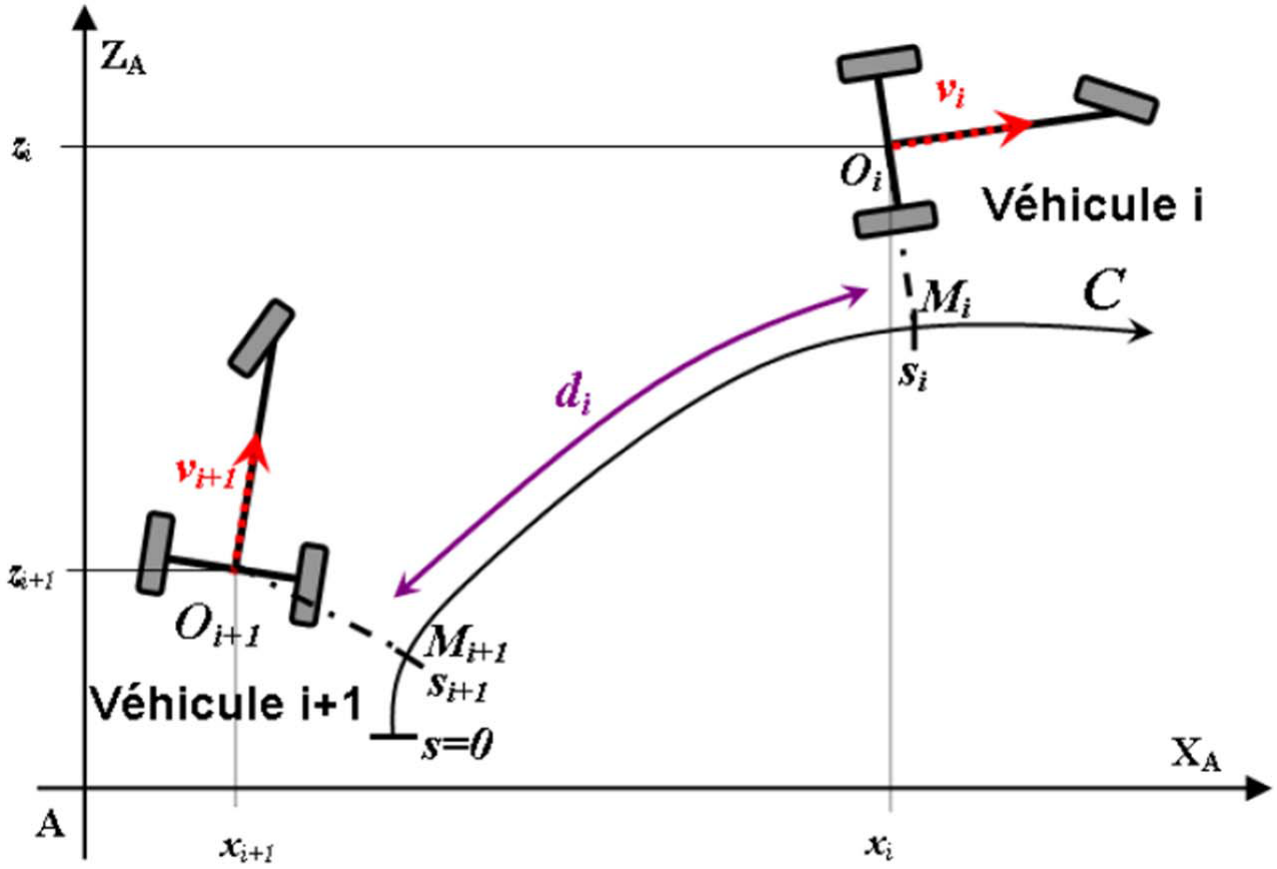

Figure 4.5: Leader-follower diagram [30]

Let us define the curved spacing error for the i^{th} vehicle as:

$$e^i_{i+1} = s_i - s_{i+1} - d$$
$$\dot{e}^i_{i+1} = \dot{s}_i - \dot{s}_{i+1}$$
$$\therefore \dot{e}^i_{i+1} = \frac{v_i.cos\tilde{\theta}_i}{1 - c(s_i)y_i} - \frac{v_{i+1}.cos\tilde{\theta}_{i+1}}{1 - c(s_{i+1})y_{i+1}}$$
$$v_{i+1} = \left(\frac{v_i.cos\tilde{\theta}_i}{1 - c(s_i)y_i} - \dot{e}^i_{i+1} \right) \frac{1 - c(s_{i+1})y_{i+1}}{cos\tilde{\theta}_{i+1}}$$
$$v_{i+1} = \frac{1 - c(s_{i+1})y_{i+1}}{cos\tilde{\theta}_{i+1}} \left(\frac{v_i.cos\tilde{\theta}_i}{1 - c(s_i)y_i} + Ke^i_{i+1} \right) \tag{4.9}$$

where we use the exponential convergence technique $\dot{e}^i_{i+1} = -k.e^i_{i+1}$ and $k > 0$.

As mentioned previously in this strategy, every vehicle is leader of the vehicle behind it (naturally everyone is leader except the last vehicle). The longitudinal control is done for each vehicle using eq. 4.10 and path-tracking or lateral control is implemented by eq. 4.1 or eq. 4.7.

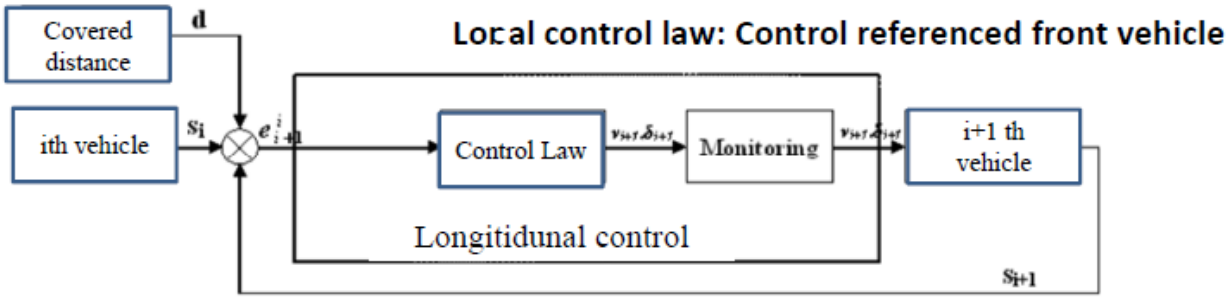

Figure 4.6: Local Control Strategy [30]

4.3.2 Global Control Strategy

In this strategy, all the vehicles of the platoon follow the leader. Consider the same notations as in figure 4.5.

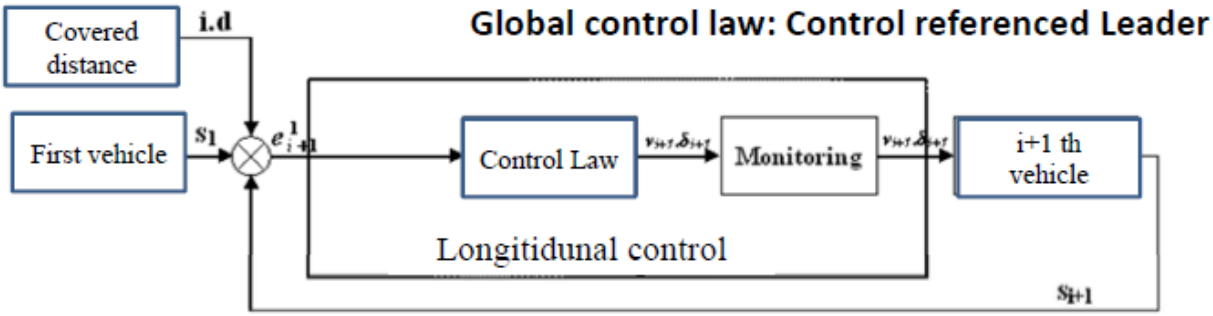

Figure 4.7: Global Control Strategy [30]

Let us define the curved spacing error for the i^{th} vehicle as:

$$e^1_{i+1} = s_1 - s_{i+1} - id$$
$$\dot{e}^1_{i+1} = \dot{s}_1 - \dot{s}_{i+1}$$

$$\therefore \dot{e}^1_{i+1} = \frac{v_1.cos\tilde{\theta}_1}{1 - c(s_1)y_1} - \frac{v_{i+1}.cos\tilde{\theta}_{i+1}}{1 - c(s_{i+1})y_{i+1}}$$

$$v_{i+1} = \left(\frac{v_1.cos\tilde{\theta}_1}{1 - c(s_1)y_1} - \dot{e}^1_{i+1} \right) \frac{1 - c(s_{i+1})y_{i+1}}{cos\tilde{\theta}_{i+1}}$$

$$v_{i+1} = \frac{1 - c(s_{i+1})y_{i+1}}{cos\tilde{\theta}_{i+1}} \left(\frac{v_1.cos\tilde{\theta}_1}{1 - c(s_1)y_1} + Ke^1_{i+1} \right) \tag{4.10}$$

where we use the exponential convergence technique $\dot{e}^1_{i+1} = -K.e^1_{i+1}$ and $K > 0$.

4.3.3 Hybrid Control Strategy

The strategies above can be combined to extract the best qualities of both. The Hybrid control strategy uses a sigmoidal function to provide coefficient weights between local and global strategy. The propagation of errors is limited but communication between leader and followers is necessary.

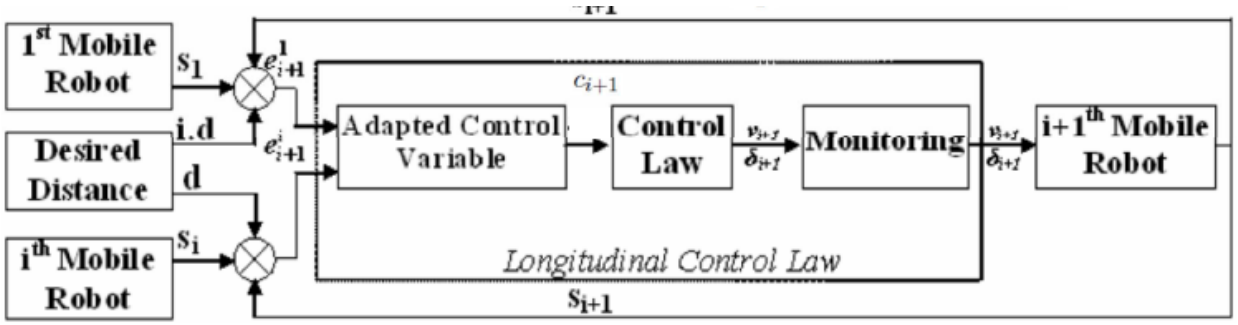

Figure 4.8: Hybrid Control Strategy [30]

The sigmoidal function is defined as:

$$\sigma_{i+1}(z_{i+1}) = \frac{1}{1 + e^{-a.z_{i+1}}} \tag{4.11}$$

where $a > 0$ and $z_{i+1} = e^i_{i+1} + \frac{d - d_s}{2}$, d_s being the minimum inter- distance.
The hybrid control law is thus defined as:

$$e_{i+1} = \sigma_{i+1} \cdot e^1_{i+1} + (1 - \sigma_{i+1}) e^i_{i+1} \tag{4.12}$$

So following the derivations used for local and global strategies in the previous sections, we can derive:

$$v_{i+1} = \sigma_{i+1} \cdot v^1_{i+1} + (1 - \sigma_{i+1}) v^i_{i+1}$$

Here the global and local control laws follow as defined:

$$v^1_{i+1} = \frac{1 - c(s_{i+1}) y_{i+1}}{cos\tilde{\theta}_{i+1}} \left(\frac{v_1 . cos\tilde{\theta}_1}{1 - c(s_1) y_1} + K e^1_{i+1} \right)$$

$$v^i_{i+1} = \frac{1 - c(s_{i+1}) y_{i+1}}{cos\tilde{\theta}_{i+1}} \left(\frac{v_i . cos\tilde{\theta}_i}{1 - c(s_i) y_i} + K e^i_{i+1} \right)$$

The implementation of the above algorithms and the inferences are provided in chapter 6 and 7.

Chapter 5

Trajectory Generation

The previous chapters portrayed an architecture to accomplish platooning of autonomous vehicles by virtue of different control strategies. However, the success of these control strategies is highly dependent on the choice of generated trajectory. Pertinent to the problem under investigation, a trajectory is an interpolating function guided by a set of control points along a path which the vehicle intends to follow. It is pretty much evident from the previous chapters that in-order to devise a control law, generated trajectory must be continuous in curvature and it's derivative. This chapter proposes a methodology which will endow the aforesaid characteristics to the trajectory

5.1 Interpolating Function

To begin with, consider a situation wherein a set of points with coordinates $\mathbf{p}_i = \begin{bmatrix} x_i & z_i \end{bmatrix}^T$ with $i = 1 \cdots N$ (where N is the total number of points) are known. These points will be henceforth referred to as control points. The goal is to formulate an interpolating function, guided by these control points, so as to ascertain continuity in curvature and it's derivative.
Following interpolating strategies were investigated during the course of project:-

1. Spline Interpolation.
2. Béizer Curves.
3. B-Splines.

B-Spline interpolation was indeed found to be appropriate for trajectory generation. The following paragraph motivates the usage of B-splines by initially invoking the limitations of former two interpolating techniques by means of small examples. It is to be noted that since these two techniques were not utilized in the project, detailed mathematical discussions, pertinent to them have not been presented. However, relevant references will be provided in-order to ascertain the completeness of results.

5.1.1 Spline Interpolation

Spline interpolation fits a polynomial function between every two successive control points. Therefore the entire trajectory is an assimilation of $N-1$ curves which are joined in such a way so as to ensure continuity in position, the first and second derivative. The total number of constraints basically decide the order and degree of polynomial function. It is completely possible to have interpolating functions of different degrees constituting a global trajectory. The set of constraints basically form a linear system of the form $\mathbf{A} \cdot \mathbf{x} = \mathbf{b}$ which can be theoretically solved. Spline interpolation is not the concern of subject under investigation and hence more details about spline interpolation and methodology to formulate a linear system can

be found on `https://people.cs.clemson.edu/~dhouse/courses/405/notes/splines.pdf`. As the number of control points increase, size of matrix A increases. During the course of project, for a set of five points interpolated with C^2 splines, size of matrix A was 18 x 18 and derivative of curvature was discontinuous at control points.

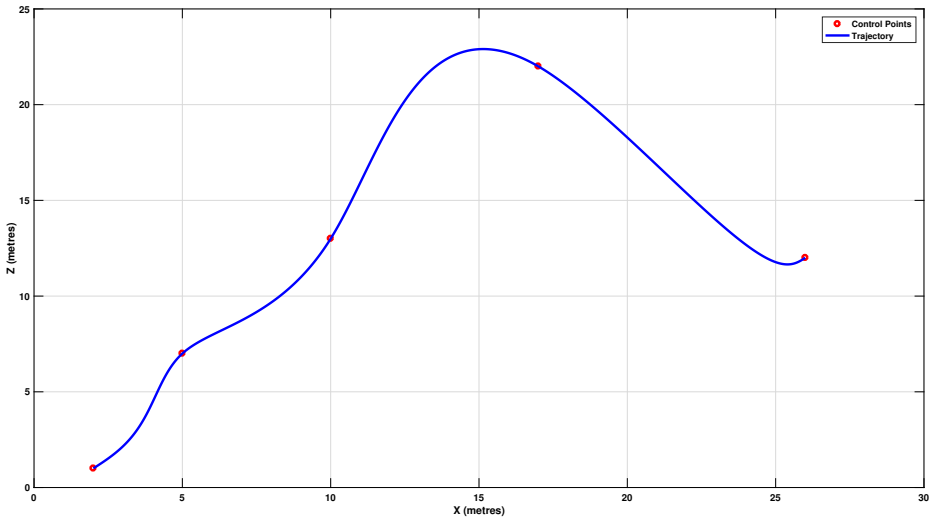

Figure 5.1: Trajectory Generation by means of Splines

The trajectory and curvature are portrayed in fig. 5.1 and 5.2. Additionally, fig. 5.3 zooms the variation of curvature and it can be seen that it is impossible to differentiate the curvature at certain values of curve parameter. The point of discontinuity is highlighted by means of vertical lines.

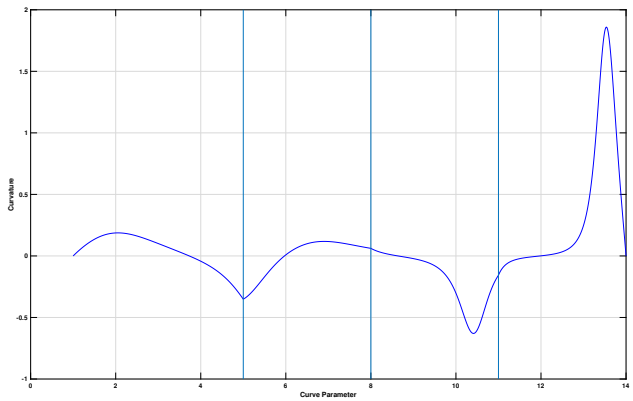

Figure 5.2: Variation of Curvature vs parameterization variable

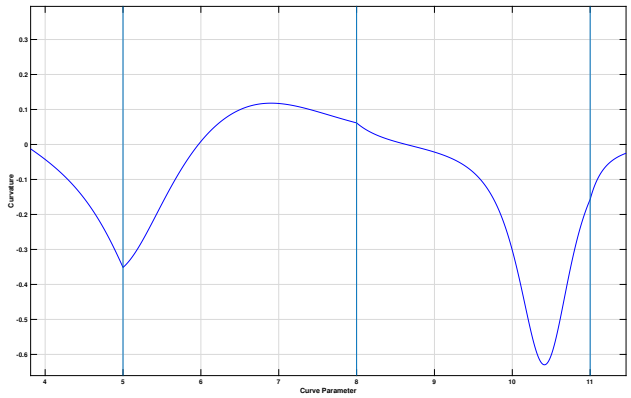

Figure 5.3: Curvature vs parameterization variable – Zoom

On adding another constraint which ensured continuity of the third derivative for a set of six points, size of matrix **A** was 28 x 28 but it was badly conditioned thereby making it close to singularity. Imagine a trajectory with over a thousand points, size of matrix **A** would be definitely large with a high degree of ill conditioning. On top of that, there is no easy way to computationally synthesize **A** matrix. However, it is not impossible to synthesize it but ill conditioning can result in poor identification of polynomial coefficients.

5.1.2 Béizer Curves

Next, Béizer curves were studied in order to fit a degree N polynomial for $N+1$ control points. The mathematical background of these curves can be accessed on `https://www.cs.mtu.edu/~shene/COURSES/cs3621/NOTES/spline/Bezier/bezier-construct.html`. A set of five control points were used to fit a degree four Béizer curve. The result is portrayed in fig. 5.4. The degree of curve that is fit is always one less than the number of control points. Imagine a situation wherein there are more than a thousand points and hence the degree of polynomial would be of the order of thousands thereby making it extremely complex. However, it is to be noted that computation of Béizer curve parameters is not as complex as formulation and solving of linear system (as in Spline interpolation).

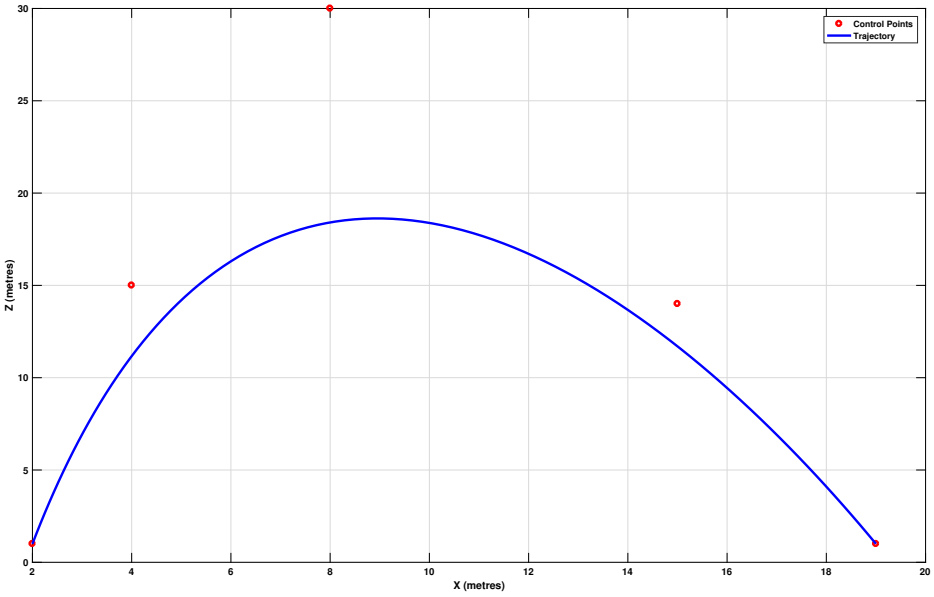

Figure 5.4: Trajectory Generation by means of Béizer Curves

Another important detail which is extremely interesting and important about Béizer curves is that there exists an internal parameter which varies from 0 to 1. This parameter frees the dependence of trajectory on a parameter associated with variation of position of point in the plane. Note that arbitrary value of parameter was chosen while implementing spline interpolation but in case of Béizer curves, no such value was chosen and indeed it was not necessary to be chosen.

5.2 B-Splines

B-Splines are generalized polynomial curves and Béizer curves are a particular type of B-Splines. To begin with consider that $N+1$ control points are known and a set of order k (degree $k-1$) curve needs to be fit in such a way that each of the *"fit-curves"* ensures C^2 continuity. Let $\mathbf{S}_g(u)$ be an interpolating function of order k varying with respect to an internal parameter $u \in [0 \quad 1]$ and $g = 1, 2, \cdots (N+1) - (k-1)$ then the interpolating function can be expressed in the the form described in Eq. (5.1).

$$\mathbf{S}_g(u) = \mathbf{u} \cdot \mathbf{M} \cdot \mathbf{p}_i \tag{5.1}$$

Note that u is the internal parameter of interpolating function where as $\mathbf{u}$ is a polynomial vector of u defined by Eq. (5.2)

$$\mathbf{u} = \begin{bmatrix} u^{k-1} & u^{k-2} & \cdots u & 1 \end{bmatrix}, \quad \mathbf{p}_i = \begin{bmatrix} x_i & y_i \\ x_{i+1} & y_{i+1} \\ \vdots & \vdots \\ x_{i+k-1} & y_{i+k-1} \end{bmatrix} \quad \text{and} \quad \mathbf{M} \in \mathbb{R}^{k \text{ x } k} \tag{5.2}$$

Note that matrix M is always constant for a given choice of order of b-spline and $i = 0, 1, 2, \cdots (k-1)$

$$\mathbf{M}_{i+1,j+1} = \frac{1}{(k-1)!} C_{k-1,i} \sum_{m=j}^{k-1} (k-(m+1))^i \ (-1)^{m-j} \ C_{k,m-j} \tag{5.3}$$

$$C_{a,b} = \frac{a!}{b!(a-b)!} \tag{5.4}$$

By utilizing the above equations, a set of (N+1)-(k-1) constituent curves of order (k-1) can

be easily generated to construct a global trajectory. The above algorithm can be easily programmed for any number of points and order without much difficulty. This is clearly advantageous as the complexity of individual curve is not as large as Béizer curves nor the computation of polynomial coefficient involves intricate programming skills.

5.3 Implementation

Theoretical paradigms, presented in the previous section, will be testified by means of numerical simulations to generate constituent curves of global trajectory. Certain characteristics particular to the trajectories are illustrated in Table 5.1

Details	Trajectory 1	Trajectory 2
Control Points	1215	1069
Degree	5	5
Order	6	6
Length	173.1433	124.7161

Table 5.1: Trajectory Details

With reference to the details above, a set of 1215 and 1069 control points were utilized to generate the trajectory shown in fig. 5.5 and fig. 5.7. A zoom of the trajectories are presented in fig. 5.6 and 5.8.

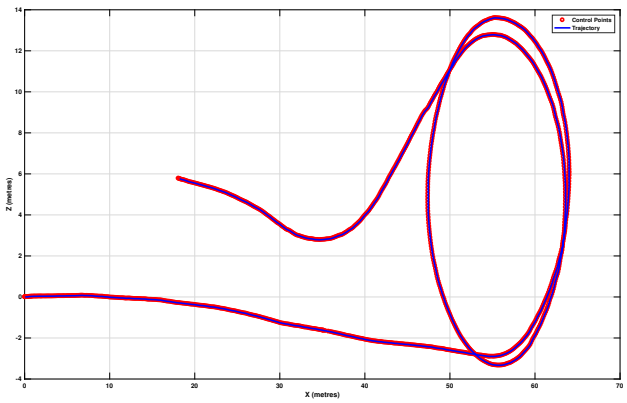

Figure 5.5: B Spline Interpolation for Trajectory 1

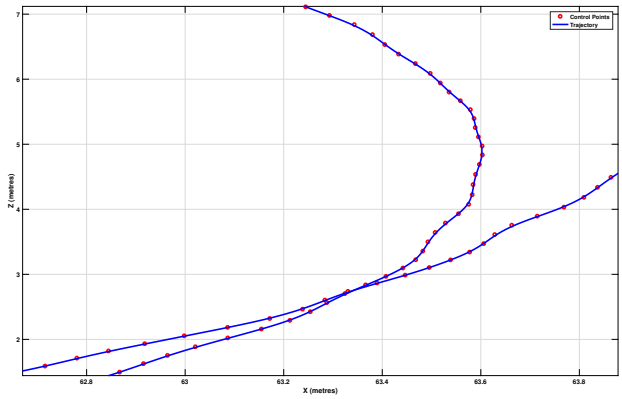

Figure 5.6: B Spline Interpolation for Trajectory 1: Zoom

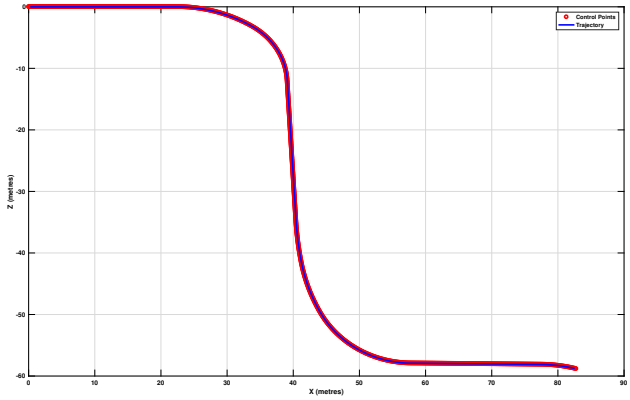

Figure 5.7: B Spline Interpolation for Trajectory 2

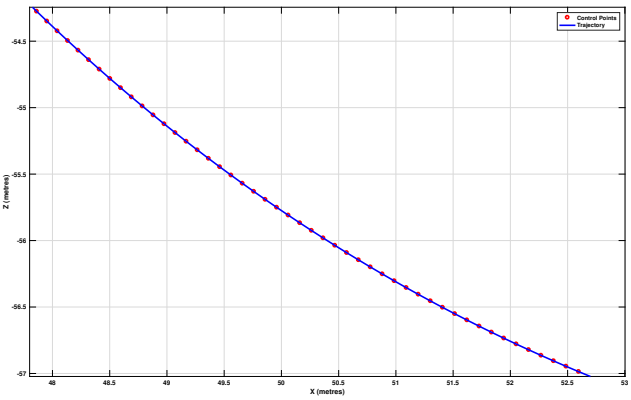

Figure 5.8: B Spline Interpolation for Trajectory 2: Zoom

5.4 Computation of Parameters for Control Law

The trajectories generated above will have to be followed by a vehicle and to do so, control strategies described in chapter 4 have to be implemented. Implementation of control law is totally dependent on computation of the following:

1. Curvilinear Abscissa: Currently the generated trajectory is composed of several constituent curves, each of them varying with respect to a local parameter as discussed earlier. The aim is to have a distinct parameter which describes the curve distinctly at each point. Curve length is chosen to be the curvilinear abscissa.

2. Foot of the perpendicular: Next is to locate a point on the generated trajectory such that a line joining located point and position of the vehicle is normal to the curve.

3. Lateral Deviation: This is basically the distance between the car and foot of perpendicular identified above.

4. Angular Deviation: Angular displacement between orientation of the vehicle and desired orientation.

5. Curvature: Finding the curvature of desired trajectory at the foot of perpendicular.

6. Derivative of Curvature with respect to curvilinear abscissa.

Computation of all these parameters will be the subject of detailed description in subsequent subsections. Note that the matrix form of trajectory, expressed in equation 5.1, can be alternatively written in the form depicted by eq. (5.5):

$$x_i^d(u) = a_{i5}u^5 + a_{i4}u^4 + a_{i3}u^3 + a_{i2}u^2 + a_{i1}u + a_{i0} \tag{5.5}$$

$$z_i^d(u) = b_{i5}u^5 + b_{i4}u^4 + b_{i3}u^3 + b_{i2}u^2 + b_{i1}u + b_{i0} \tag{5.6}$$

$$\tag{5.7}$$

The above form can be compactly written as

$$\mathbf{r}_i(u) = \begin{bmatrix} x_i^d(u) & z_i^d(u) \end{bmatrix}^T \tag{5.8}$$

5.4.1 Curve Length

Mathematically, curve length or arc length is defined as

$$s_i(u) = \int_0^u \|\mathbf{r}_i'(q)\|_2 \, dq \tag{5.9}$$

Note that the expression $r'(q)$ is tangent vector associated with curve $r(q)$. Also, the value of parameter u is known to vary from 0 to 1 for all the constituent curves. The above equation will therefore provide a numerical value of lengths of each individual curve which can be cumulatively added to find the curvilinear abscissa associated with end points of each constituent curve.

5.4.2 Foot of the perpendicular

As discussed in chapter 3, point M on the trajectory is such that a line joining this point and location of vehicle is normal to the trajectory. In fact, depending on the nature of trajectory there could be several such points on the trajectory which are normal to the trajectory (for different values of s). To start with, M has smallest possible value of s such that the above discussed condition is met. As the vehicle moves forward, point M is chosen such that curvilinear abscissa (s) associated with it is at least as large as the previous value of s. Jumping to mathematical jargon: for a particular given instant, let $\mathbf{p} = [x \quad y]^T$ be the location of vehicle with M lying on the trajectory and therefore satisfying eq. (5.5). By imposing the condition of orthogonality, following relation can be obtained:

$$\vec{PM}^T \cdot \mathbf{r}'(u) = 0 \tag{5.10}$$

$$[x^d(u) - x] \cdot x'^d(u) + [y^d(u) - y] \cdot y_i'^d(u) = 0 \tag{5.11}$$

The above eq. (5.10) simplifies to a degree 9 polynomial of the form

$$\begin{bmatrix} u^9 & u^8 & \cdots & 1 \end{bmatrix} \cdot [\mathbf{a} + \mathbf{b}] = 0 \tag{5.12}$$

The intermediate vectors **a** and **b** are defined as

$$\mathbf{a} = \begin{bmatrix} 5 * a_5 * a_5 \\ 4 * a_4 * a_5 + 5 * a_5 * a_4 \\ 3 * a_3 * a_5 + 4 * a_4 * a_4 + 5 * a_5 * a_3 \\ 2 * a_2 * a_5 + 3 * a_3 * a_4 + 4 * a_4 * a_3 + 5 * a_5 * a_2 \\ 1 * a_1 * a_5 + 2 * a_2 * a_4 + 3 * a_3 * a_3 + 4 * a_4 * a_2 + 5 * a_1 * a_5 \\ 1 * a_1 * a_4 + 2 * a_2 * a_3 + 3 * a_3 * a_2 + 4 * a_1 * a_4 + 5 * a_5 * (a_0 - x) \\ 1 * a_1 * a_3 + 2 * a_2 * a_2 + 3 * a_1 * a_3 + 4 * a_4 * (a_0 - x) \\ 1 * a_1 * a_2 + 2 * a_1 * a_2 + 3 * a_3 * (a_0 - x) \\ 1 * a_1 * a_1 + 2 * a_2 * (a_0 - x) \\ 1 * a_1 * (a_0 - x) \end{bmatrix}$$

$$\mathbf{b} = \begin{bmatrix} 5 * b_5 * b_5 \\ 4 * b_4 * b_5 + 5 * b_5 * b_4 \\ 3 * b_3 * b_5 + 4 * b_4 * b_4 + 5 * b_5 * b_3 \\ 2 * b_2 * b_5 + 3 * b_3 * b_4 + 4 * b_4 * b_3 + 5 * b_5 * b_2 \\ 1 * b_1 * b_5 + 2 * b_2 * b_4 + 3 * b_3 * b_3 + 4 * b_4 * b_2 + 5 * b_1 * b_5 \\ 1 * b_1 * b_4 + 2 * b_2 * b_3 + 3 * b_3 * b_2 + 4 * b_1 * b_4 + 5 * b_5 * (b_0 - y) \\ 1 * b_1 * b_3 + 2 * b_2 * b_2 + 3 * b_1 * b_3 + 4 * b_4 * (b_0 - y) \\ 1 * b_1 * b_2 + 2 * b_1 * b_2 + 3 * b_3 * (b_0 - y) \\ 1 * b_1 * b_1 + 2 * b_2 * (b_0 - y) \\ 1 * b_1 * (b_0 - y) \end{bmatrix}$$

Note that the symbol * denotes multiplication. On solving eq. (5.12), value of u can be found. If $u = u_M$ is found to be a real number lying between 0 and 1 then there exists a point M with coordinates (x_M, y_M) on the constituent curve under focus. In case there doesn't exist a valid point M then it is necessary to move to subsequent constituent curves until a valid point is found.

5.4.3 Lateral Deviation

Lateral deviation can be computed by utilizing the following relation:

$$y = \sqrt{(x_M - x)^2 + (y_M - y)^2} \tag{5.13}$$

5.4.4 Angular Deviation

Angular deviation is given by:

$$\tilde{\theta} = \theta - \theta^d \tag{5.14}$$

Note that θ^d can be computed by using the following relation:

$$\theta^d = \arctan \frac{y'^d(u_M)}{x'^d(u_M)}$$

5.4.5 Curvature

Curvature is computed using the following relation:

$$c = \frac{x'(u_M)y''(u_M) - y'(u_M)x''(u_M)}{(x'(u_M)^2 + y'(u_M)^2)^{3/2}} \tag{5.15}$$

5.4.6 Derivative of Curvature

To implement the control law, it is necessary to compute the derivative of curvature with respect to curvilinear abscissa and not local parameter u. Thus a plausible way to compute the

derivative would be to use the chain rule:

$$\frac{dc}{ds} = \frac{dc}{du} \cdot \frac{du}{ds} \tag{5.16}$$

Note that relation connecting s and u is given by eq. 5.9 and it is extremely difficult to analytically formalize an expression relating s and u and thus the derivative will be computed numerically by using the following relation:

$$\frac{dc}{ds}(s_M) = \frac{c(s_M + \delta) - c(s_M - \delta)}{2\delta} \tag{5.17}$$

With this all necessary parameters for implementing the control law have been discussed which were the requirements to accomplish successfu control system design. The next chapter will be dedicated to implementing all the theoretical formulations developed in the previous chapters.

Chapter 6

Simulation

This chapter is dedicated to presentation of results obtained on simulating the proposed localization module for a degree five polynomial trajectory guided by a given set of control points for existing control strategies based on PD Control.

The trajectory 1, described in table 5.1, is used as a reference trajectory to be followed. All the paradigms which were presented in the previous chapters have been used exclusively for carrying out simulation studies. The findings of previous chapters will be recalled from time to time to emphasize the correctness of implementation.

A rudimentary investigation on the accuracy of tracking with PD and Sliding Mode Control under influence of perturbations has also been performed for completeness.

6.1 Lateral Control

This section throws light on implementation of classical lateral control presented in chapter 4 for the localization module postulated in this report. Prior knowledge of trajectory aides the transformation of Cartesian coordinates and orientation to curvilinear distance, lateral and angular deviation. These three entities form the basis of localization module and other parameters, like curvature and derivative of curvature, needed for control signal generation (as discussed in chapter 5). As the dynamics of transformed state variables vary with respect to curvilinear distance (chapter 4), introduction of control drives the lateral and angular deviation to zero as curvilinear distance goes to ∞. The results presented in fig. 6.2 testify the purported claim thereby leading to *very exact* tracking of reference path as shown in fig. 6.3. Note that an angular deviation of 2π or 4π are basically equivalent to zero. The control signals to bring about the desired action is presented in fig. 6.1. Note that since lateral and longitudinal controls are decoupled, therefore, choice of longitudinal speed is independent of steering angle . This is completely evident from the presented results, where in a variable velocity profile was used to track the reference trajectory. The experimental parameters pertinent to the simulation are tabulated in Table 6.1

Parameter	Value
Proportional Gain (K_p)	25
Derivative Gain (K_d)	10
Wheel base	1 m
Initial position	$[2\ \ 2]^T$ m
Initial orientation	0.5 rad

Table 6.1: Simulation Details: Lateral Control

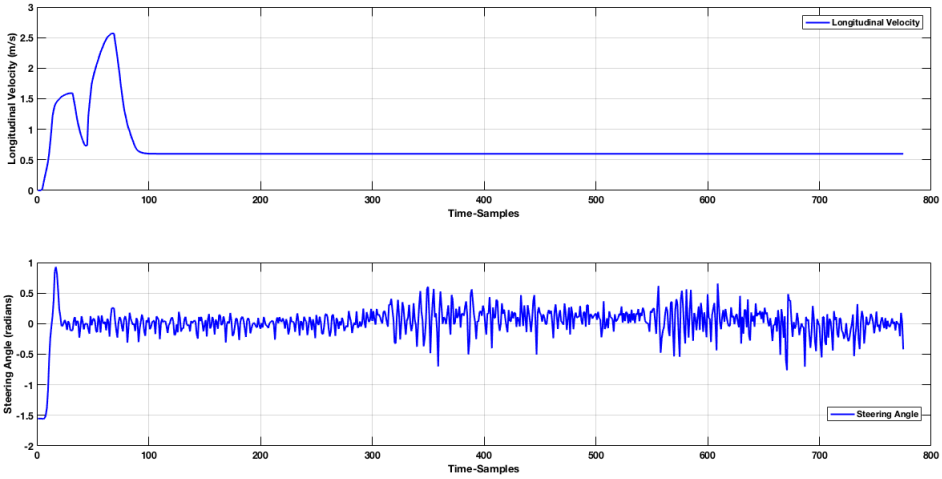

Figure 6.1: Lateral Control: Control signal

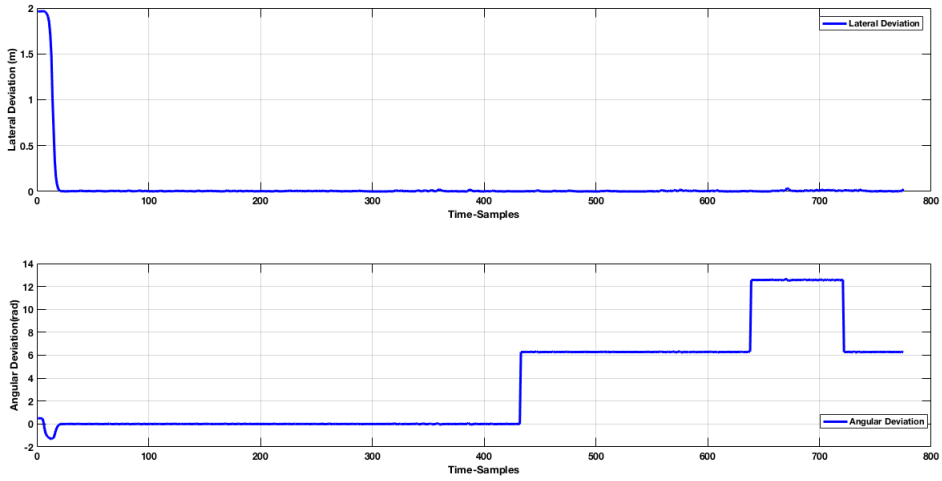

Figure 6.2: Lateral Control: Lateral and Angular Deviations

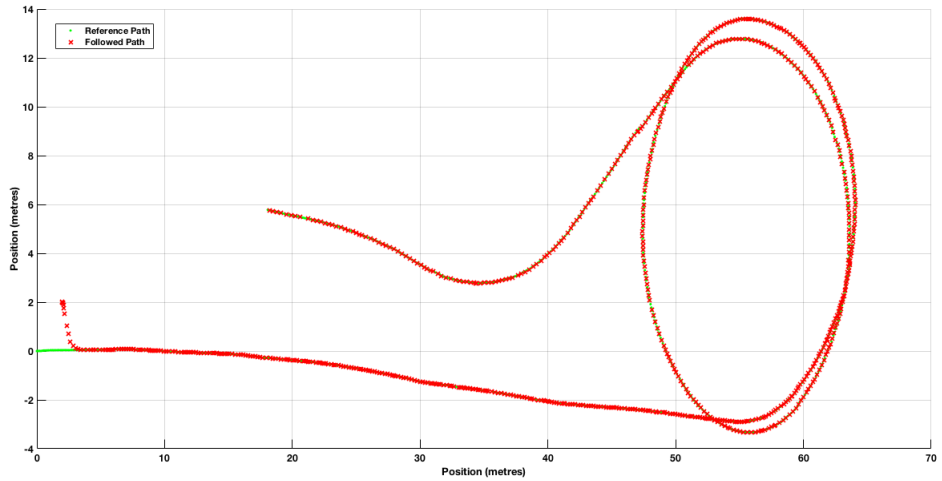

Figure 6.3: Lateral Control:Path

6.2 Longitudinal Control

The lateral controller discussed above was responsible for manipulating steering angle of the vehicle whereas longitudinal control maintains the heading speed of the vehicle in-order to maintain a specified inter-vehicular distance between the immediate leader and follower. The longitudinal control law described in chapter 4 was implemented for a system comprising of one leader and a follower. Both lateral and longitudinal controllers were implemented to drive the lateral and angular variations to 0 and spacing between vehicles to a specified distance of 1 m. The presented results are in concurrence with the theory postulated in the report and it can be seen from fig. 6.5 that lateral and angular deviations of both the vehicles approach zero as curvilinear distance increases. Secondly as the two vehicles are initialized somewhat far from each other a spike in the longitudinal speed of the follower can be observed, as shown in fig. 6.4. The longitudinal curvilinear distance between the two vehicles settles at 1m as shown in fig. 6.7 and traversed path is depicted in fig. 6.6. The values of gains and parameters pertinent to the simulation are presented in table 6.2

Parameter	Value
Proportional Gain (Lateral) (K_p)	25
Derivative Gain (Lateral) (K_d)	10
Wheel base	1 m
Initial position (Leader)	$[10 \;\; 2]^T$ m
Initial orientation (Leader)	0 rad
Initial position (Leader)	$[2 \;\; 1]^T$ m
Initial orientation (Leader)	0 rad
Proportional gain K (Longitudinal)	5
Desired inter-distance (d)	1 m

Table 6.2: Simulation Details: Longitudinal Control

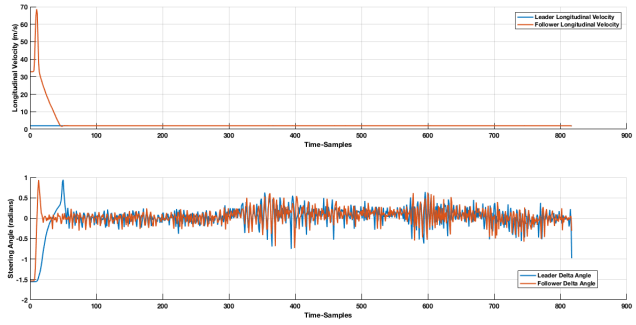

Figure 6.4: Leader Follower: Control signal

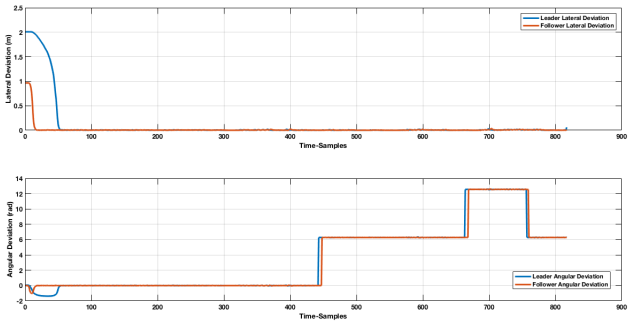

Figure 6.5: Leader Follower: Lateral and Angular Deviations

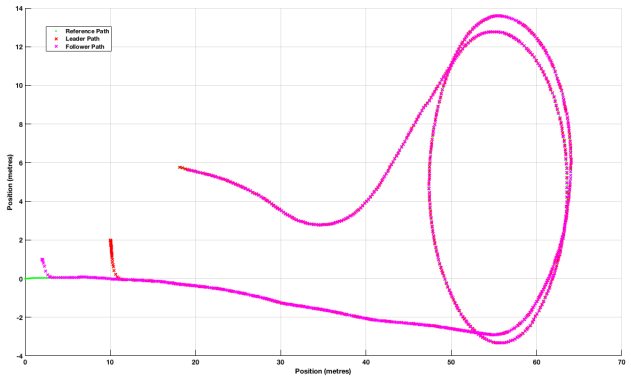

Figure 6.6: Leader Follower: Path

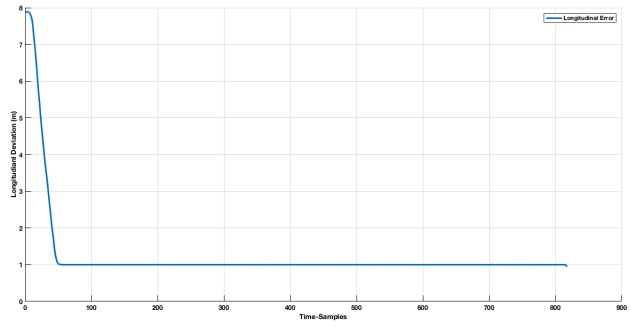

Figure 6.7: Leader Follower: Longitudinal Curvilinear distance between vehicles

6.3 Local Control of Platoon

We simulate a platoon of 5 vehicles using a local control strategy as described in chapter 4. The simulink model is designed as in fig 6.8. It is evident that the longitudinal velocity control depends on the curvilinear distance between the current vehicle and the vehicle in front.

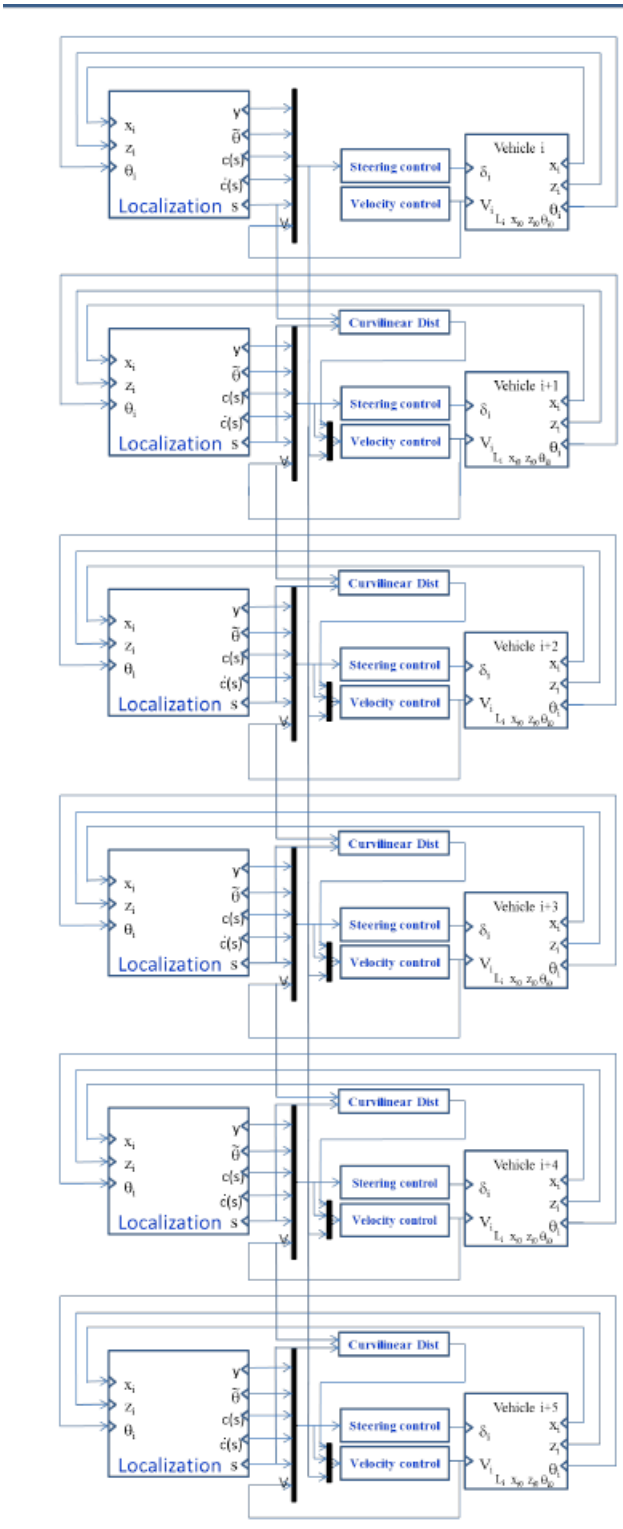

Figure 6.8: Simulink model: Local control [30]

The design parameters are tabulated below:

Parameter	Value
Proportional Gain (Lateral) (K_p)	25
Derivative Gain (Lateral) (K_d)	10
Wheel base	1 m
Initial position (Leader)	$[6\ \ 1]^T$ m
Initial orientation (Leader)	0 rad
Initial position (Follower 1)	$[5\ \ 1]^T$ m
Initial orientation (Follower 1)	0 rad
Initial position (Follower 2)	$[4\ \ 1]^T$ m
Initial orientation (Follower 2)	0 rad
Initial position (Follower 3)	$[3\ \ 1]^T$ m
Initial orientation (Follower 3)	0 rad
Initial position (Follower 4)	$[2\ \ 1]^T$ m
Initial orientation (Follower 4)	0 rad
Proportional gain K (Longitudinal)	5
Desired inter-distance (d)	1 m

Table 6.3: Simulation Details: Local Control Strategy

The results show clearly that convergence in lateral and longitudinal errors is preserved. The longitudinal curvilinear distance between the vehicles converges to the constant spacing of 1m as seen from 6.12. Figure 6.10 shows that all the vehicles track the path desired and the settling time is around 20s. The fact that this is a local strategy makes it necessary to ensure good communication of among the vehicles because each follower should know the state of its leader. The five vehicles have a proposed initial state and show a good tracking of the trajectories.

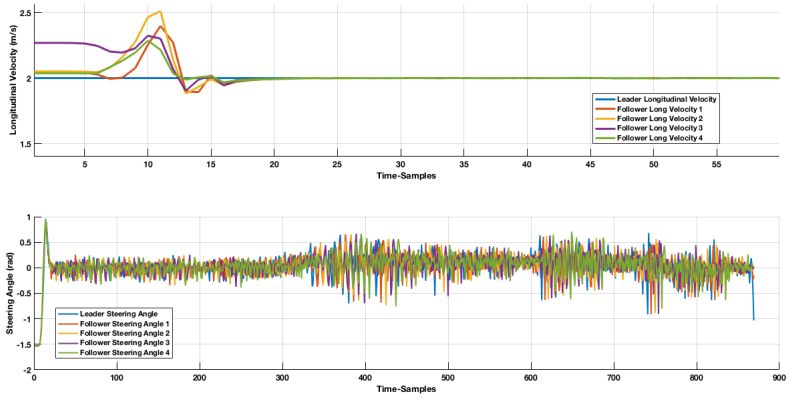

Figure 6.9: Local Platoon Control: Control signal

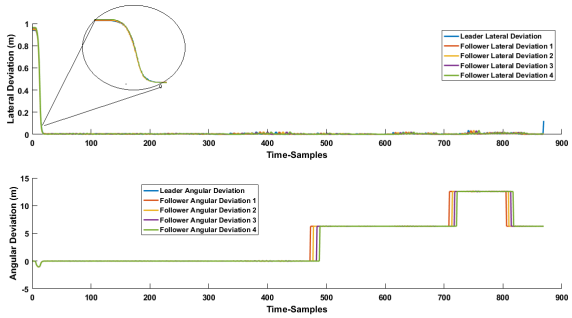

Figure 6.10: Local Platoon Control: Lateral and Angular Deviations

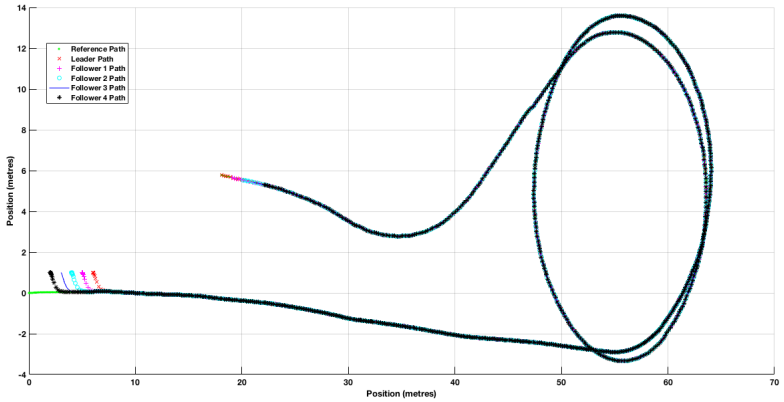

Figure 6.11: Local Platoon Control: Path

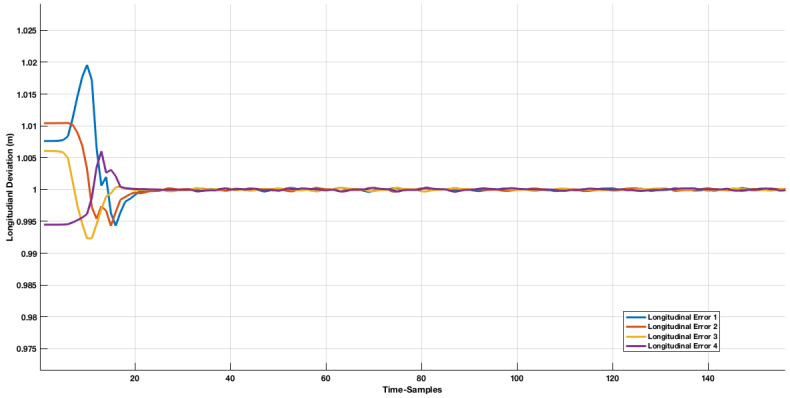

Figure 6.12: Local Platoon Control: Longitudinal Curvilinear distance between vehicles

6.3.1 Fault Tolerance

It is interesting to see what happens if one of the follower vehicles fails/stops. In fig 6.13 at around T=1100 samples we intentionally put the longitudinal velocity of follower vehicle 3 to 0. It can be seen that the longitudinal deviation increases as the vehicle in front of follower 3 reaches the desired destination. The longitudinal deviation for follower vehicle 4 remains same as it is calculated between vehicle 3 and vehicle 4. Follower vehicle 4 also stops at 1m distance

behind follower vehicle 3. This shows that in local control strategy, if one vehicle in the platoon is affected, all the vehicles behind it are also affected as seen in fig 6.14.

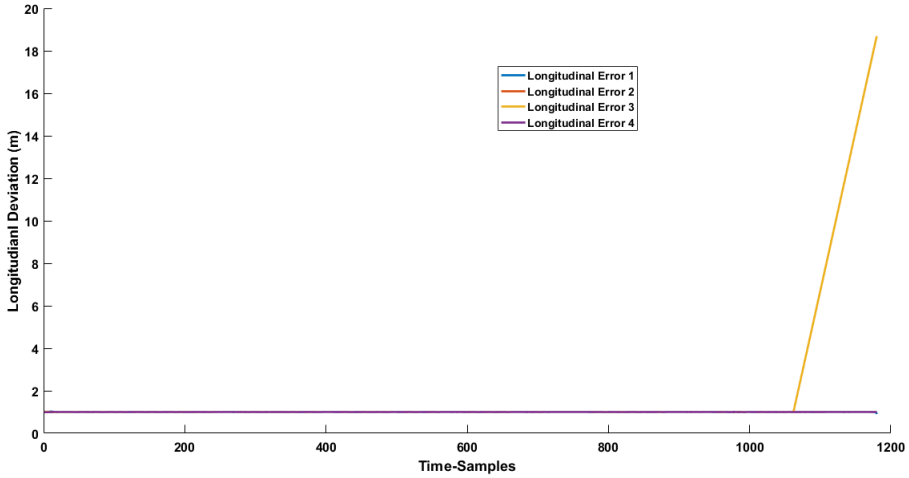

Figure 6.13: Local Platooning failure: Longitudinal Deviation

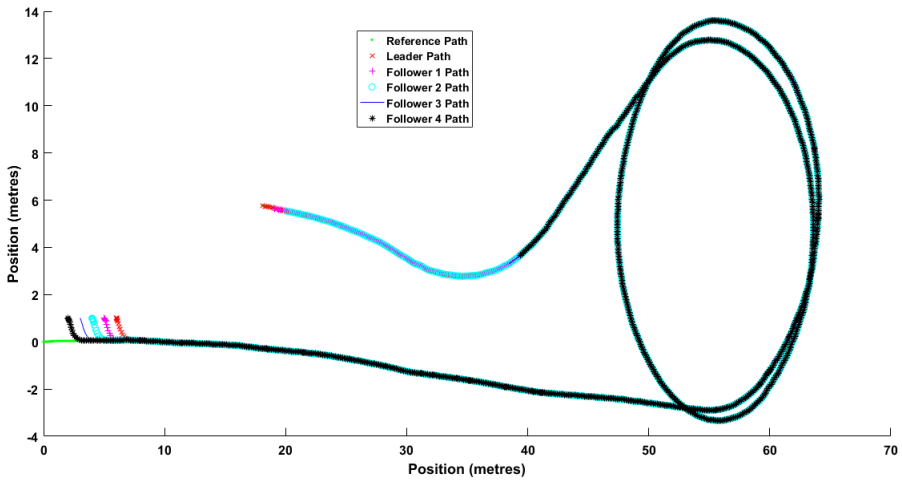

Figure 6.14: Local Platooning failure: Path

6.4 Global Control of Platoon

In global strategy, longitudinal velocity control is derived using the curvilinear distance of follower vehicle from the leader vehicle as described in chapter 4.

The design parameters for Global control strategy are tabulated below:

Parameter	Value
Proportional Gain (Lateral) (K_p)	25
Derivative Gain (Lateral) (K_d)	10
Wheel base	1 m
Initial position (Leader)	$[10\ \ 1]^T$ m
Initial orientation (Leader)	0 rad
Initial position (Follower 1)	$[7\ \ 1]^T$ m
Initial orientation (Follower 1)	0 rad
Initial position (Follower 2)	$[5\ \ 1]^T$ m
Initial orientation (Follower 2)	0 rad
Initial position (Follower 3)	$[4\ \ 1]^T$ m
Initial orientation (Follower 3)	0 rad
Initial position (Follower 4)	$[2\ \ 1]^T$ m
Initial orientation (Follower 4)	0 rad
Proportional gain K (Longitudinal)	5
Desired inter-distance (d)	2 m

Table 6.4: Simulation Details: Global Control Strategy

As it can be seen from the fig 6.18, the curvilinear inter-distance between the vehicles is dependent only on the leader vehicles so we notice some oscillations. The longitudinal error settles to 1m inter-distance at around 40s and lateral error settles at around 35s.

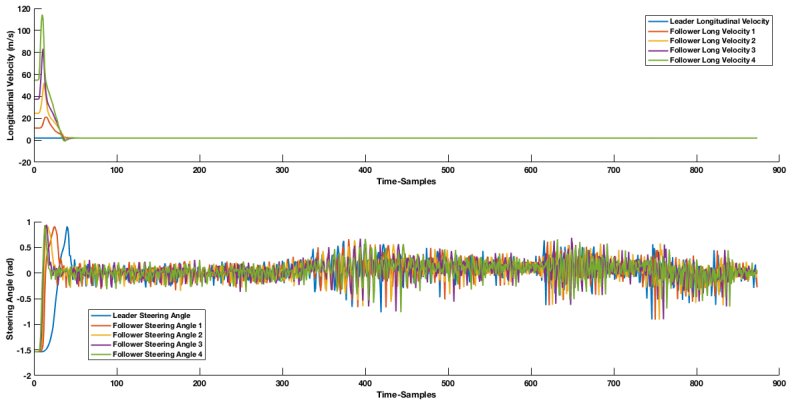

Figure 6.15: Global Control of Platoon: Control signal

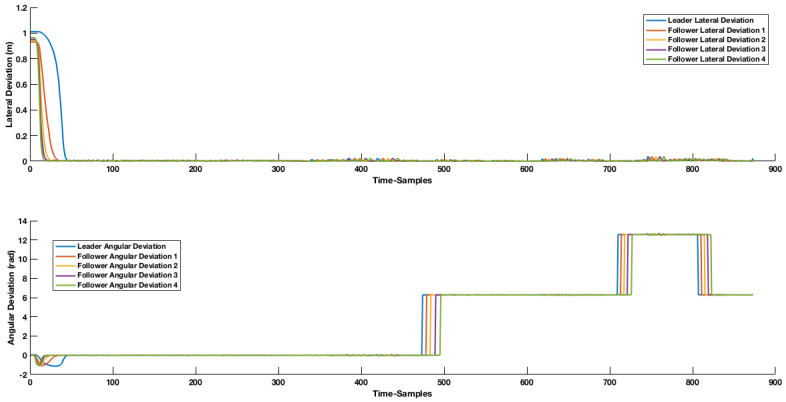

Figure 6.16: Global Control of Platoon: Lateral and Angular Deviations

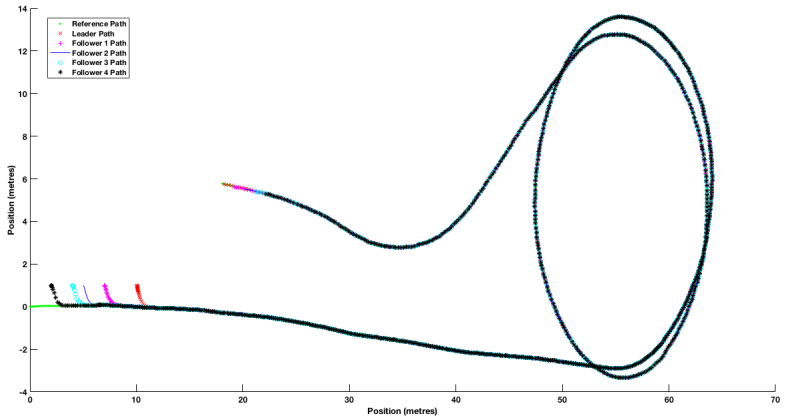

Figure 6.17: Global Control of Platoon: Path

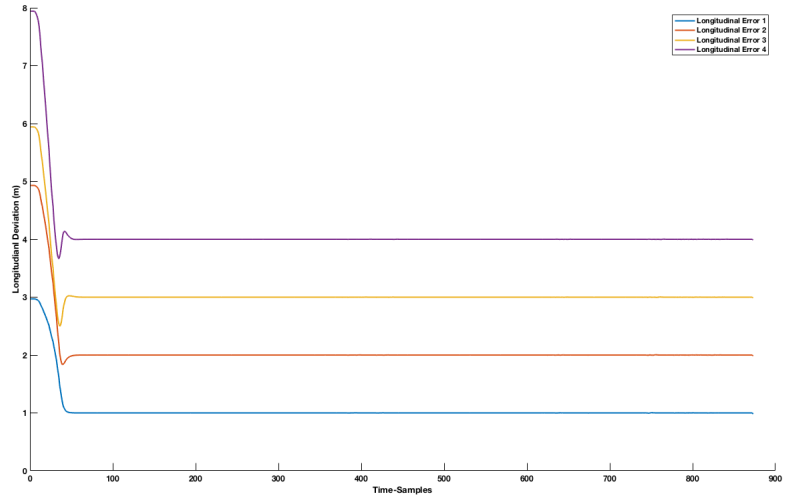

Figure 6.18: Global Control of Platoon: Longitudinal Curvilinear distance between follower and leader

6.4.1 Fault Tolerance

In the global strategy, there is no propagation of errors since the control is derived directly from the leader. But the communication between the leader and the followers must be highly trusted.
As in local strategy, we intentionally stop the follower vehicle 3 after some time. In contrast to local case, the vehicle 4 goes past the vehicle 3 and reaches the destination as in fig 6.20. We can see from fig 6.19 the longitudinal deviation for vehicle3 increases after it stops and vehicle4 settles at a distance of 2m from the vehicle2 which is as expected. This may be a major issue if there is no safety process (obstacle avoidance) installed in the cars as a sudden stop may cause collisions.

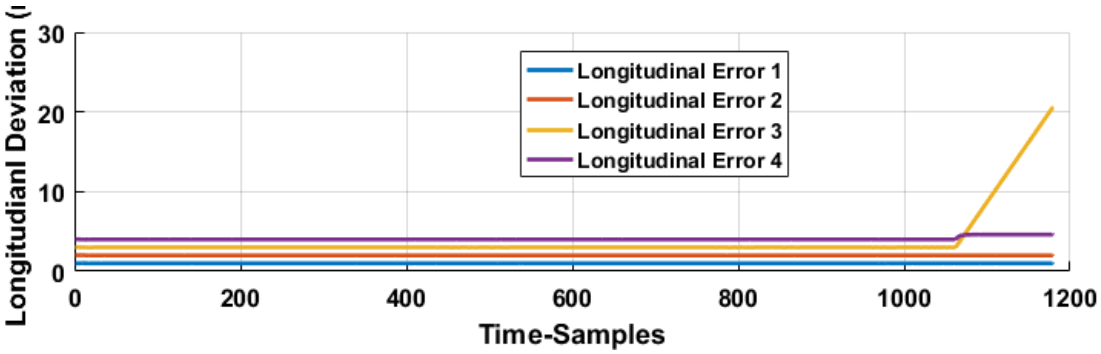

Figure 6.19: Longitudinal Deviation

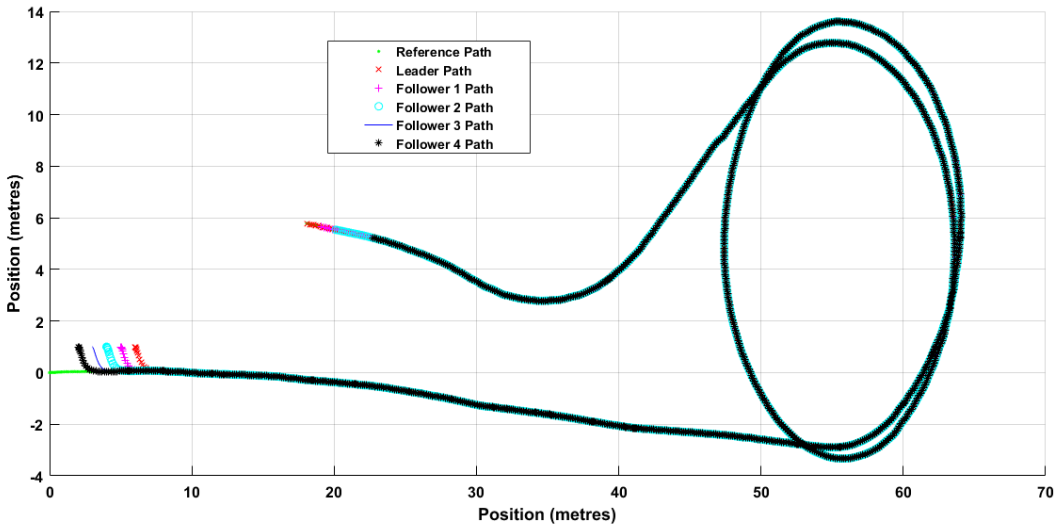

Figure 6.20: Path

6.5 Hybrid Control of Platoon

Every vehicle is follower of the vehicle in the front and of the vehicle at the beginning of the queue in a controlled manner. For this sigmoid functions have to be used as in chapter 4. Notice that both local and global control laws will be used but the longitudinal control law will be regulated by the distance of each vehicle with respect to the vehicle in the front. If this distance is small, the local control law will be more likely to be applied and vice versa for the global control law.

The design parameters are tabulated below:

Parameter	Value
Proportional Gain (Lateral) (K_p)	25
Derivative Gain (Lateral) (K_d)	10
Wheel base	1 m
Initial position (Leader)	$[10\ \ 1]^T$ m
Initial orientation (Leader)	0 rad
Initial position (Follower 1)	$[7\ \ 1]^T$ m
Initial orientation (Follower 1)	0 rad
Initial position (Follower 2)	$[5\ \ 1]^T$ m
Initial orientation (Follower 2)	0 rad
Initial position (Follower 3)	$[4\ \ 1]^T$ m
Initial orientation (Follower 3)	0 rad
Initial position (Follower 4)	$[2\ \ 1]^T$ m
Initial orientation (Follower 4)	0 rad
Proportional gain K (Longitudinal)	5
Desired inter-distance (d)	2 m
Minimum inter-distance (ds)	0.5
sigmoid parameter a	2

Table 6.5: Simulation Details: Hybrid Control Strategy

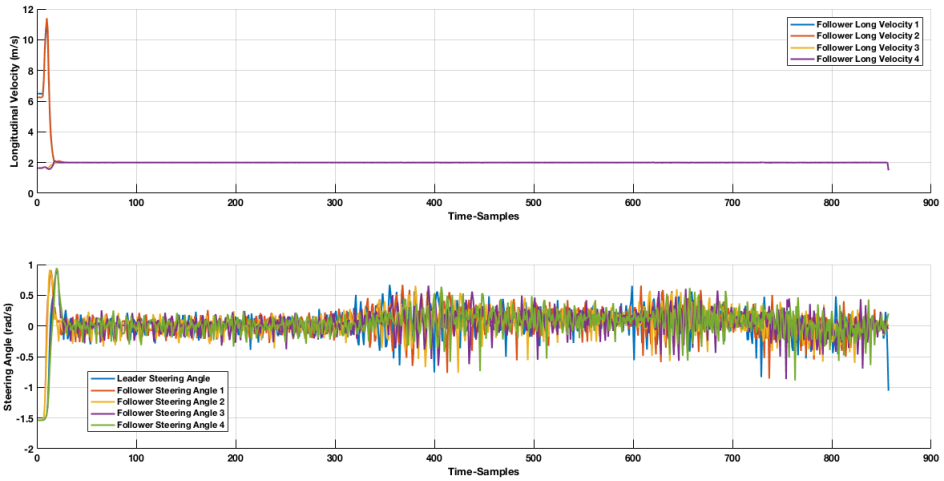

Figure 6.21: Hybrid Control of Platoon: Control signal

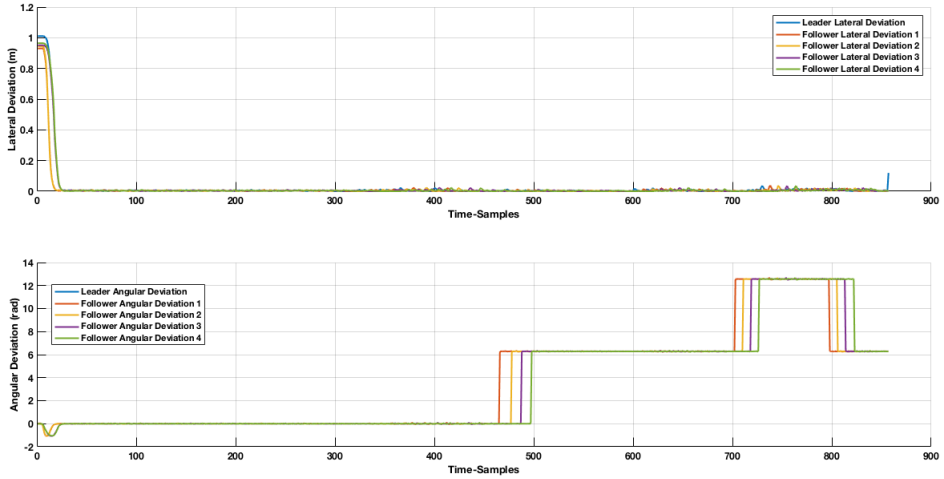

Figure 6.22: Hybrid Control of Platoon: Lateral and Angular Deviations

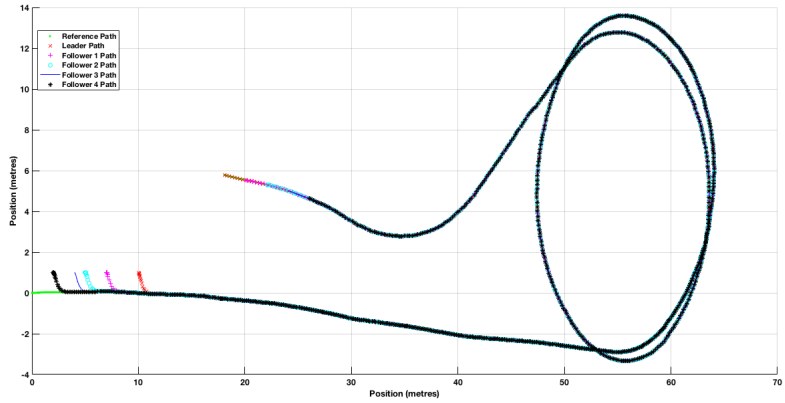

Figure 6.23: Hybrid Control of Platoon: Path

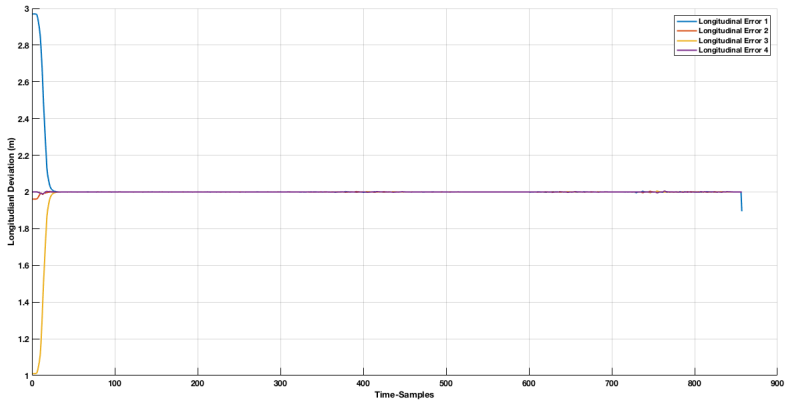

Figure 6.24: Hybrid Control of Platoon: Longitudinal Curvilinear distance between vehicles

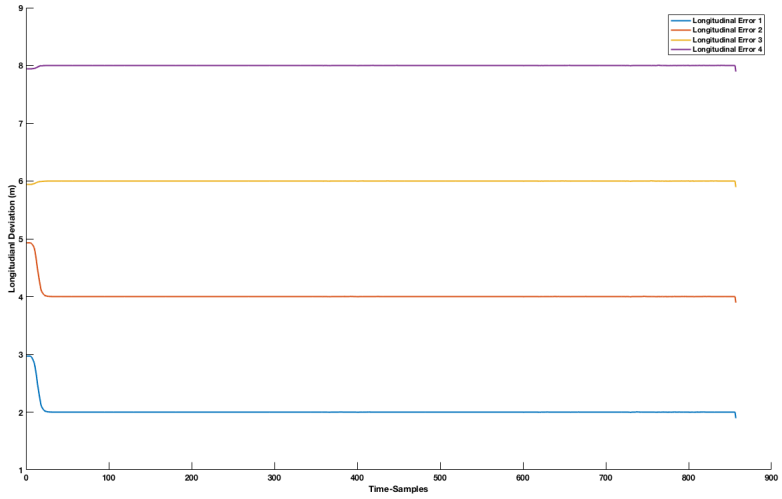

Figure 6.25: Hybrid Control of Platoon: Distance of follower vehicles from the leader.

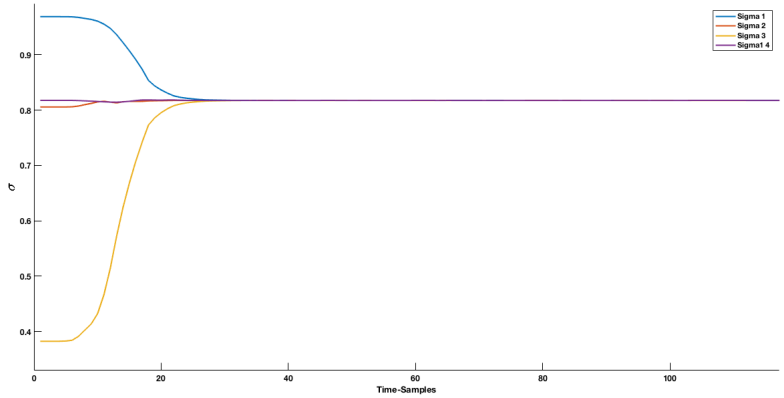

Figure 6.26: Hybrid Control of Platoon: Variation of σ

Figure 6.24 shows the longitudinal curvilinear distance between the platoon vehicles and fig 6.25 shows the longitudinal curvilinear distance between the followers and the leader. The evolution of σ shows that the distances are initially intermediate values between d and id but as we approach settling time, the intermediate distances all converge to approximately $d = 2m$.

6.5.1 Fault Tolerance

We now intentionally put the follower vehicle3 to rest after some time and check the behaviour of the vehicle4.

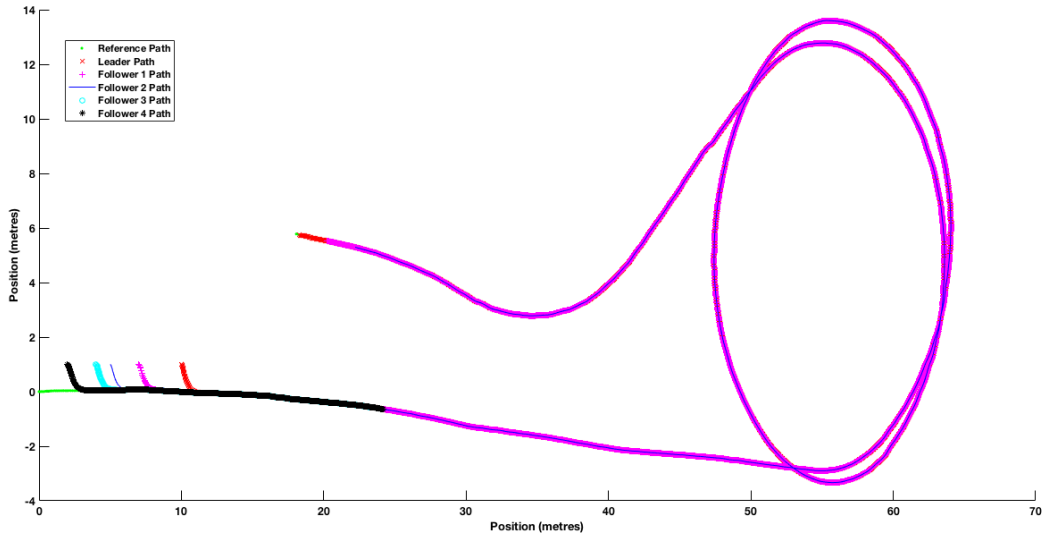

Figure 6.27: Path

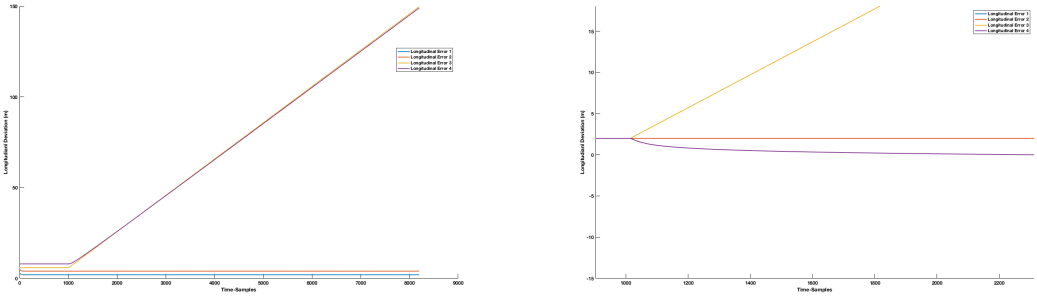

(a) Longitudinal distance to leader

(b) Longitudinal distance between followers

The `vehicle4` stops just after vehicle3 stops showing the effect of local control as can be seen from the fig 6.27, 6.28a and 6.28b. The distance to the leader increases monotonically for `vehicle3` and `vehicle4` and the inter-distance between `vehicle3` and `vehicle4` settles at an intermediate value $d < 2m$. So we can infer that hybrid control combines the best of both worlds from local and global control laws.

6.6 Perturbation Analysis

The hardware is not ideal as modelled in our simulations. Here we present a brief perturbation analysis to show the juxtaposition between Sliding Mode Controller(SMC) and Classical PD Controller for Lateral control. We implement for lateral control case as sliding mode is highly robust in tracking problems in case of perturbations. The longitudinal control case can be satisfactorily controlled by a proportional controller as it involves minimization of an error.

Lets consider two types of perturbation:

- A one shot error in GPS data for the localisation causing a shift in readings 6.29b.
- A uniform random number data signal in the localisation data between $\pm 10cm$ for outdoor purposes as in fig 6.29a. We can use $\pm 50cm$ for industrial purposes with cheap sensors but here we assume we have good quality sensor readings.

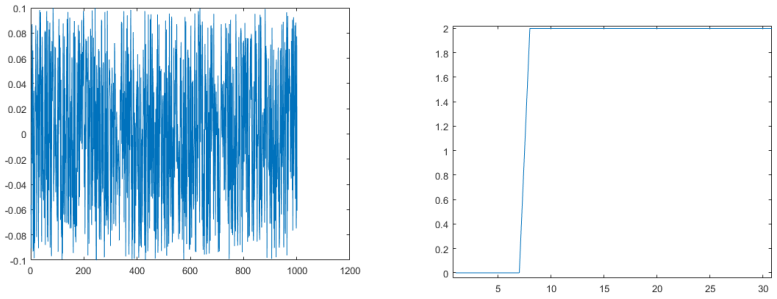

(a) Uniform random number noise

(b) One shot error

Figure 6.29: Pertubations

We get the following plots with a one shot error with a PD Controller and Sliding mode controller:

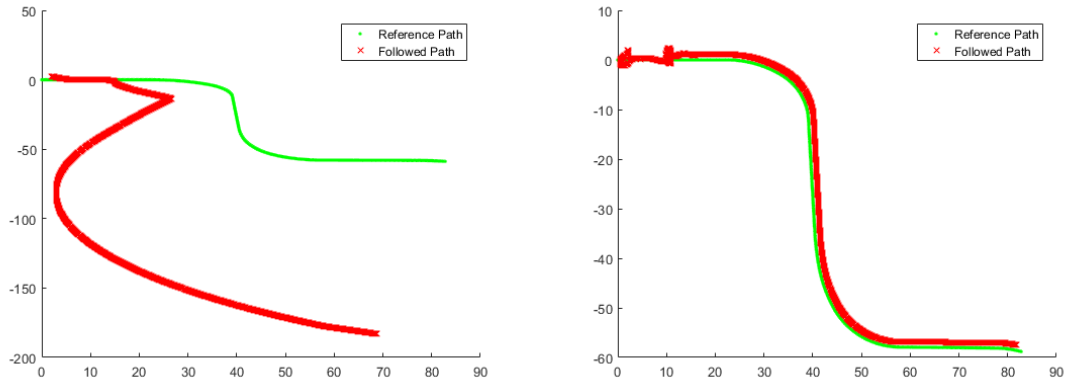

(a) PD controller with perturbation

(b) Sliding mode controller with perturbation

Figure 6.30

We see clearly that the PD controller is not able to track the path while the Sliding mode controller is more efficient in tracking. We must however note that PD controller can be tuned to provide satisfactory results but results in higher gains which may be physically improbable or the frequencies associated with the gains can affect the actuators.

We get the following plots with a uniform random noisy input between $\pm 10cm$ with a PD Controller and Sliding mode controller:

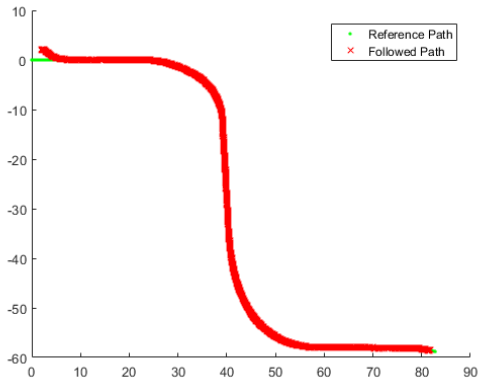

(a) PD controller with perturbation

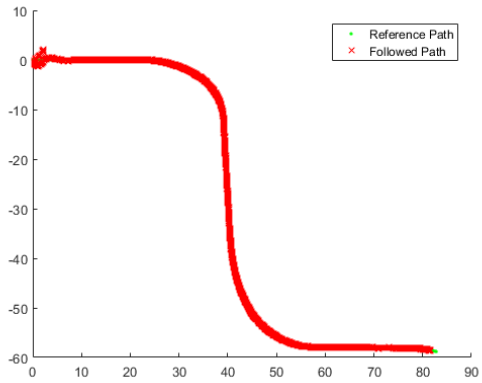

(b) Sliding mode controller with perturbation

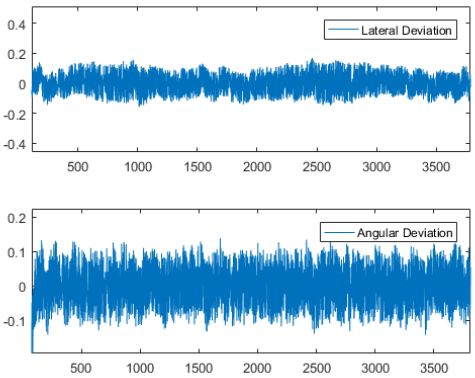

(c) PD controller with perturbation

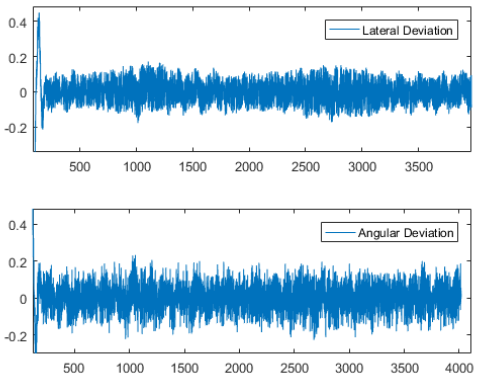

(d) Sliding mode controller with perturbation

Figure 6.31

In this case, however the difference is not very clear as both controllers react effectively for a uniform random noise input.

There is however a classical problem when using a first order sliding mode controller which is the chattering effect as in fig 6.32b. The high chattering causes damage to the actuators.

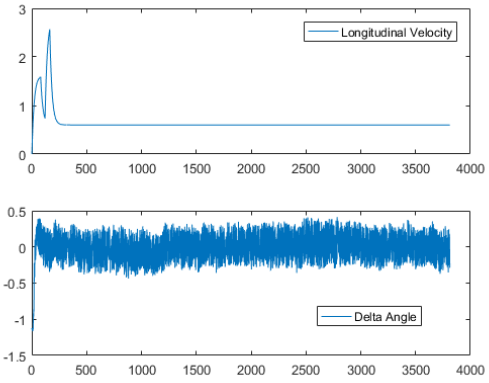

(a) PD controller with perturbation

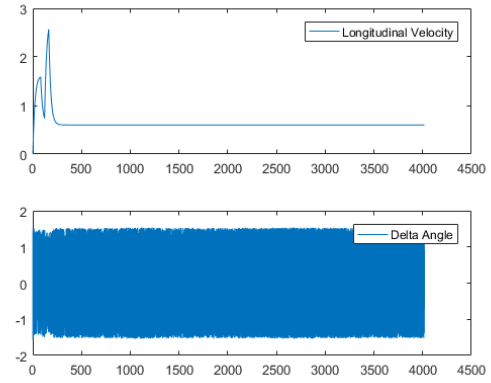

(b) Sliding mode controller with perturbation

Figure 6.32

6.7 ADAMS Visualization

We used ADAMS to visualize the lateral control of one vehicle. No dynamic modelling or analysis was done using ADAMS, but rather just used as a visualization tool.

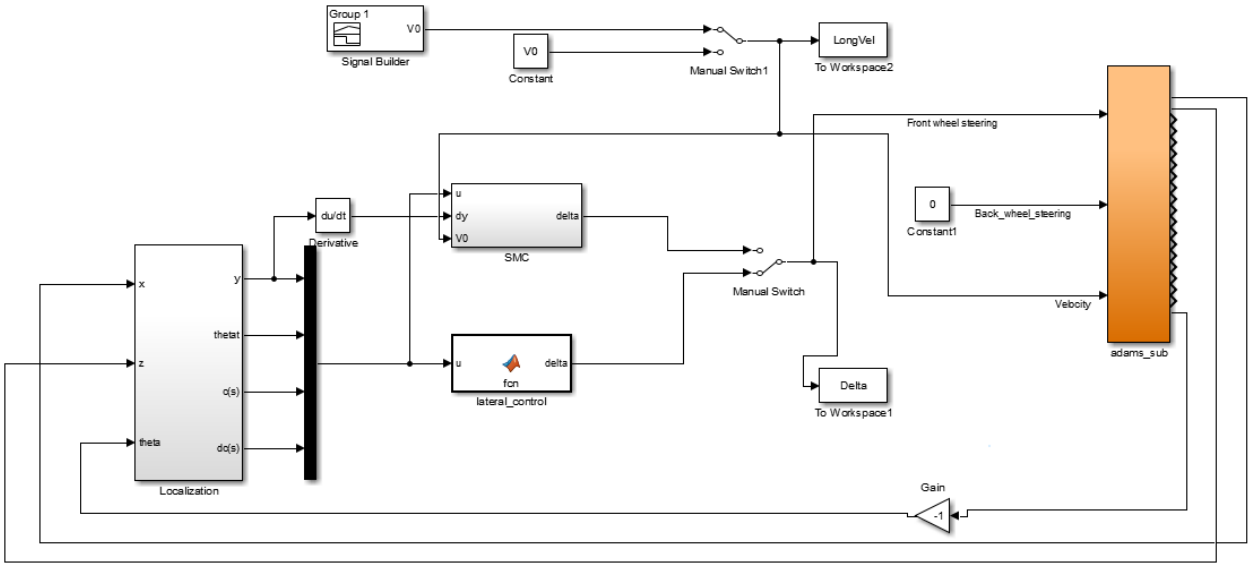

Figure 6.33: ADAMS in Simulink model

The `adams_sub` block in the SIMULINK diagram in fig 6.33 replaces the bicycle model and uses a car model in ADAMS. It has many elements to simulate contact forces with the ground, gravity, speed and orientation measuring units and so on. The car-model can be seen in figure 6.34. The simulation for tracking the trajectory `trajZAdams` (6.31d) is show in fig 6.35, 6.36 and 6.37.

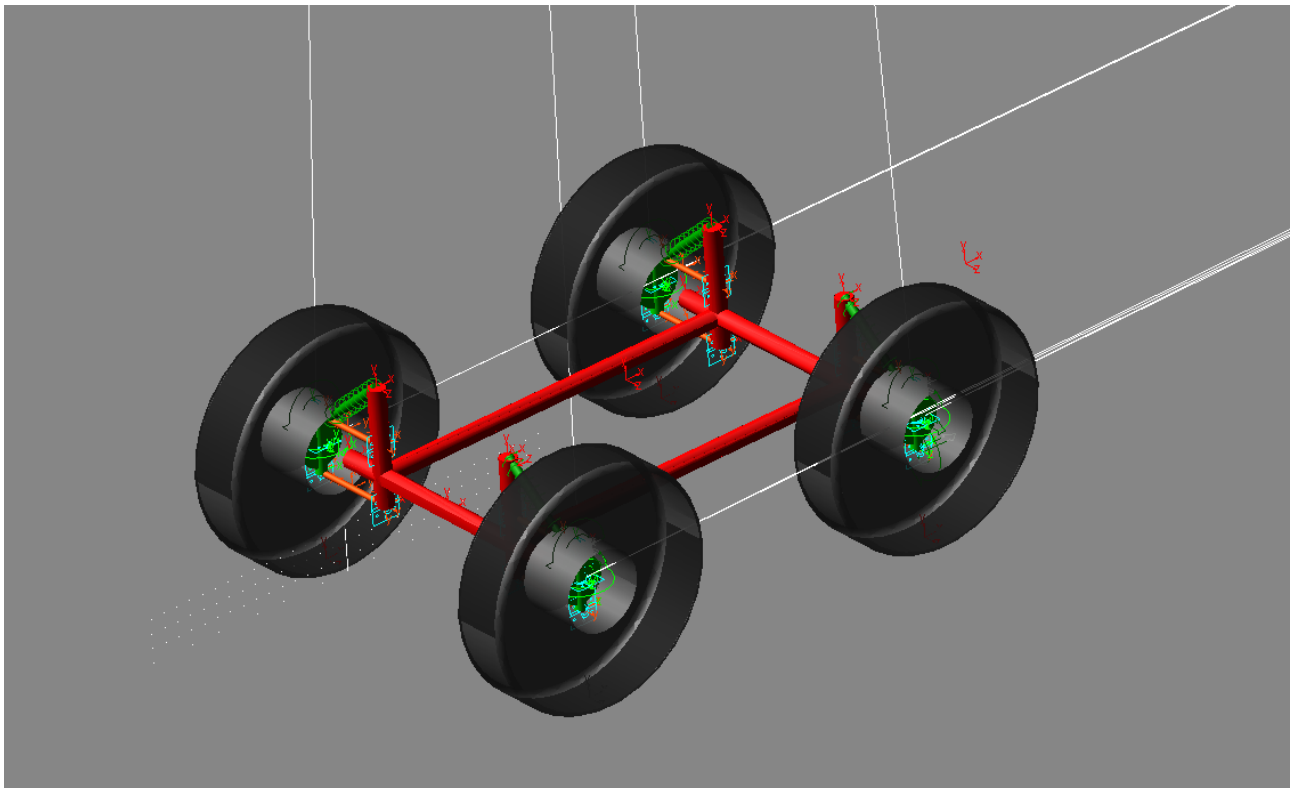

Figure 6.34: ADAMS Model

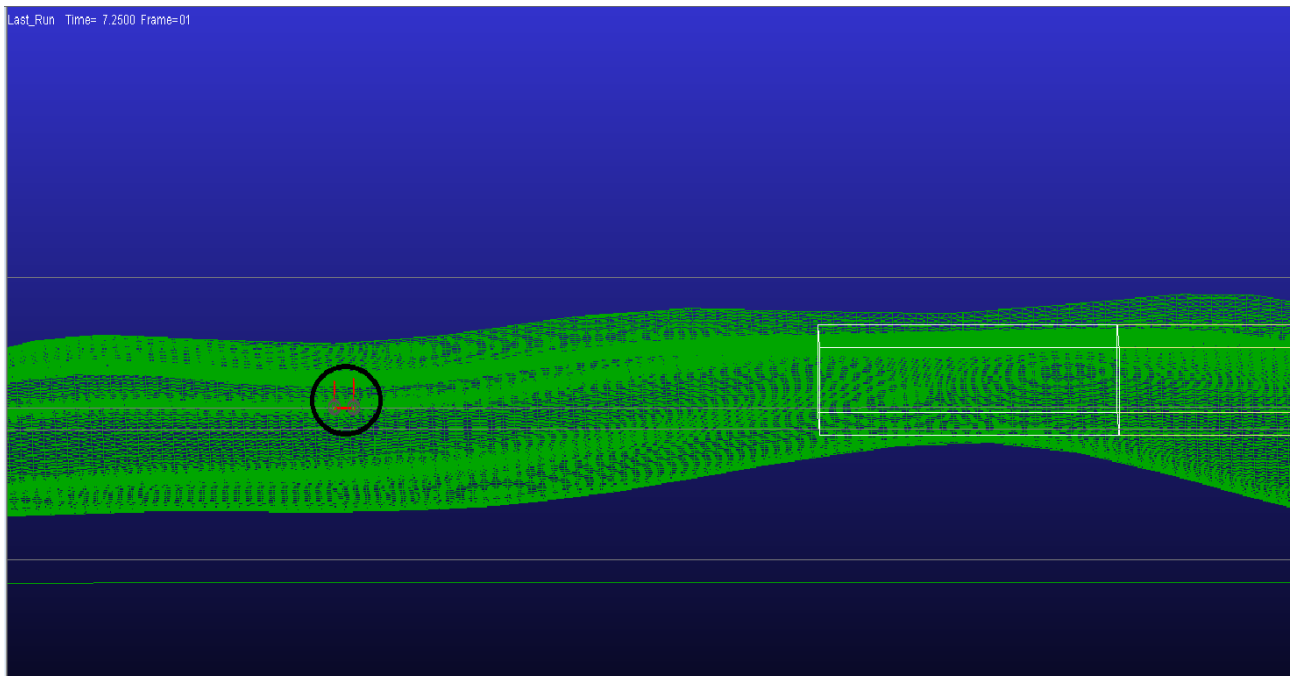

Figure 6.35: ADAMS Simulation

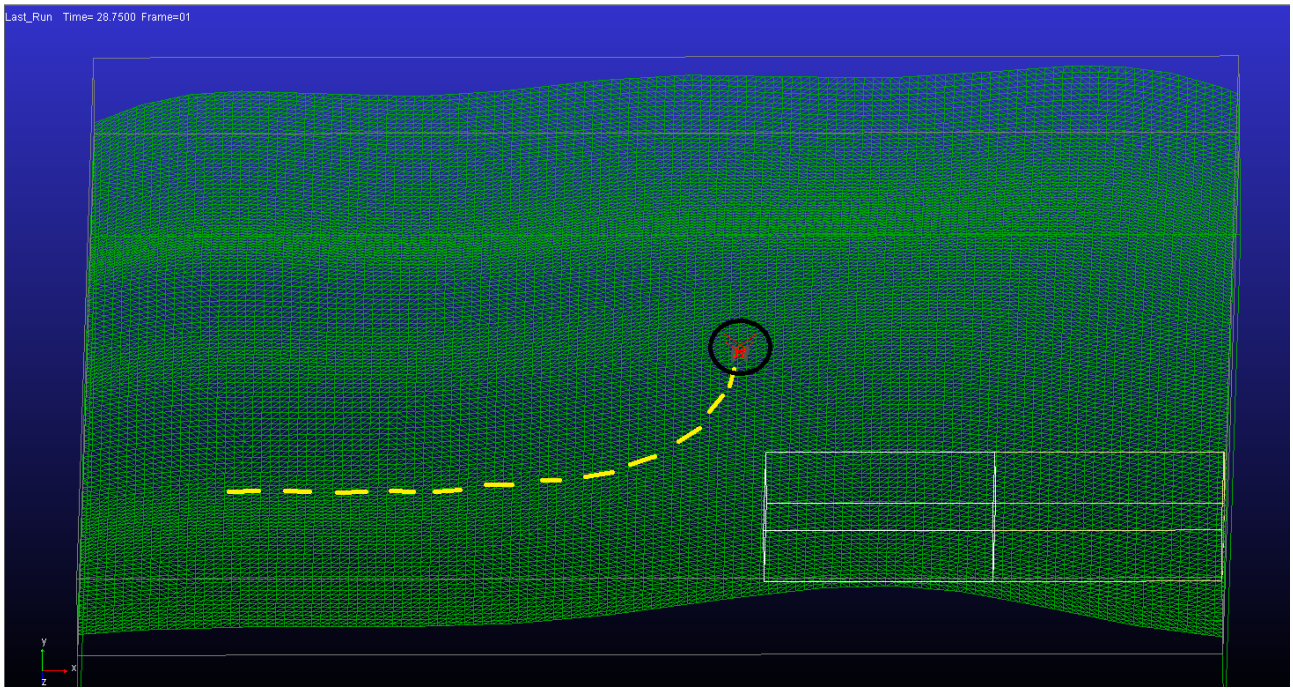

Figure 6.36: ADAMS Simulation

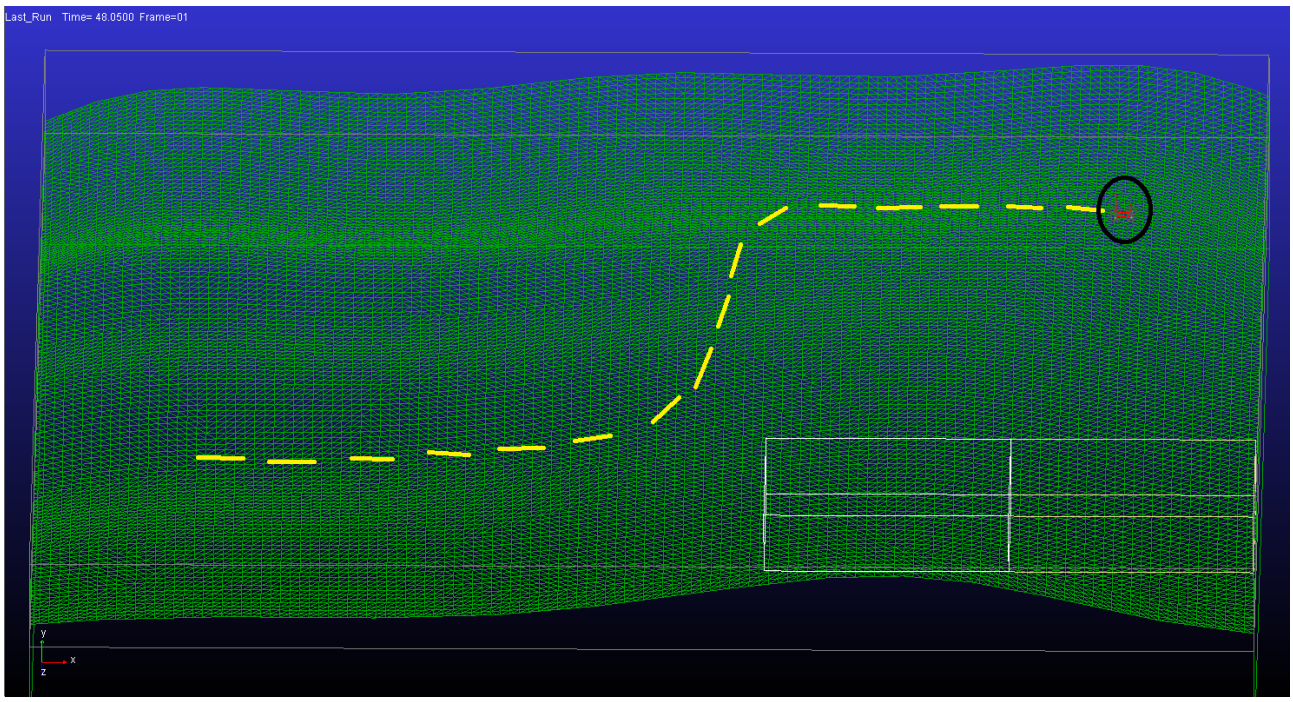

Figure 6.37: ADAMS Simulation

Chapter 7

Conclusion and Discussion

The presented work primarily focused on modelling and control of a platoon of autonomous vehicles. The project commenced with study and implementation of kinematics of a vehicle in Frènet frame. Control of a System modelled in Frènet frame necessitates generation of a trajectory which is at-least C^2 that is continuous in curvature. In order to build a trajectory, from the pre-existing set of points, B-Spline interpolation of order six (that is degree 5) was utilized. Using a degree five polynomial ensured high degree of smoothness which was highly desirable. This smoothness and continuity indeed facilitated computation of curvature and it's derivative. The work purported computation of curvilinear abscissa with a high degree of accuracy which was utilized to obtain lateral deviation, angular deviation, curvature and it's derivative. These computations indeed facilitated smooth implementation of existing control strategies in-order to accomplish tracking of a desired trajectory. MATLAB/SIMULINK was utilized to testify the veracity of localization module proposed in the project. The proposed module was tested for a trajectory generated from a set of 1215 distinct points by using 1210 constituent curves of degree five each, connected together in continuity. The control law was found to be successfully driving the lateral deviation, angular deviation to zero and inter-distance between vehicles was found to be maintained at a specified distance. Observed simulation results were found to be in complete concurrence with the theoretical and mathematical formulations presented in the report. The proposed localization block was then imbibed in local, global and hybrid control architecture and as expected, satisfactory results were obtained. By means of simulation study, the merits of utilizing a hybrid control architecture over former two topologies were underscored i.e. propagation errors of errors is limited and safety is enhanced at an expense of robust communication system. On the other hand,for local strategy only data from adjacent data is needed but propagation of errors increases from one vehicle to the other. The global control strategy however has no error propagation as leader transmits the same data to all the followers but any minor crash in this communication would lead to complete collapse of the system thereby compromising with the safety. For sake of completeness, a brief perturbation analysis of the PD controller and Sliding mode controller was implemented for the lateral control law. We infer in case of tracking problems with inherent perturbations, the first order sliding mode controller is better than the PD controller with a trade-off on the chattering effect on the inputs.

7.1 Future Work

Tuning of gains was observed to be highly dependent on the nature of path and hence it was not possible to generate an online trajectory. In future, the findings of this project may be extended with an adaptive control strategy so as to accomplish platooning for a initially unknown path (by the leader). The effect of sliding were ignored and tyre to road contact was assumed to be a single point. The communication delays were not considered anywhere in the analysis. Additionally, it was assumed that all geometric parameters were known with exact accuracy whereas in real life it might not be the case. The sensor induced noises were not studied during

the project and in real life each sensor induces different noise. This type of situation may be difficult to model. All the aafore-mentioned conditions may be studied in the future to check the performance of proposed localization module.

Bibliography

[1] B. Thuilot, J. Bom, F. Marmoiton, and P. Martinet, "Accurate automatic guidance of an urban electric vehicle relying on a kinematic gps sensor," in *5th IFAC Symposium on Intelligent Autonomous Vehicles (IAV'04)*, 2004.

[2] S. Sheikholeslam and C. A. Desoer, "Combined longitudinal and lateral control of a platoon of vehicles," in *American Control Conference, 1992*, pp. 1763–1767, IEEE, 1992.

[3] P. Daviet and M. Parent, "Longitudinal and lateral servoing of vehicles in a platoon," in *Intelligent Vehicles Symposium, 1996., Proceedings of the 1996 IEEE*, pp. 41–46, IEEE, 1996.

[4] R. Rajamani, H.-S. Tan, B. K. Law, and W.-B. Zhang, "Demonstration of integrated longitudinal and lateral control for the operation of automated vehicles in platoons," *IEEE Transactions on Control Systems Technology*, vol. 8, no. 4, pp. 695–708, 2000.

[5] S. Mammar, V. B. Baghdassarian, and L. Nouveliere, "Speed scheduled vehicle lateral control," in *Intelligent Transportation Systems, 1999. Proceedings. 1999 IEEE/IEEJ/JSAI International Conference on*, pp. 80–85, IEEE, 1999.

[6] A. Ali, G. Garcia, and P. Martinet, "Urban platooning using a flatbed tow truck model," in *Intelligent Vehicles Symposium (IV), 2015 IEEE*, pp. 374–379, IEEE, 2015.

[7] G. Tagne, R. Talj, and A. Charara, "Higher-order sliding mode control for lateral dynamics of autonomous vehicles, with experimental validation," in *Intelligent Vehicles Symposium (IV), 2013 IEEE*, pp. 678–683, IEEE, 2013.

[8] S. Chaib, M. S. Netto, and S. Mammar, "H ∞, adaptive, pid and fuzzy control: a comparison of controllers for vehicle lane keeping," in *Intelligent Vehicles Symposium, 2004 IEEE*, pp. 139–144, IEEE, 2004.

[9] P. Zhao, J. Chen, Y. Song, X. Tao, T. Xu, and T. Mei, "Design of a control system for an autonomous vehicle based on adaptive-pid," *International Journal of Advanced Robotic Systems*, vol. 9, no. 2, p. 44, 2012.

[10] J. M. Snider *et al.*, "Automatic steering methods for autonomous automobile path tracking," *Robotics Institute, Pittsburgh, PA, Tech. Rep. CMU-RITR-09-08*, 2009.

[11] T. Hessburg and M. Tomizuka, "Fuzzy logic control for lateral vehicle guidance," *IEEE Control Systems*, vol. 14, no. 4, pp. 55–63, 1994.

[12] R. Lenain, B. Thuilot, C. Cariou, and P. Martinet, "High accuracy path tracking for vehicles in presence of sliding: Application to farm vehicle automatic guidance for agricultural tasks," *Autonomous robots*, vol. 21, no. 1, pp. 79–97, 2006.

[13] S. Benhimane, E. Malis, P. Rives, and J. R. Azinheira, "Vision-based control for car platooning using homography decomposition," in *Robotics and Automation, 2005. ICRA 2005. Proceedings of the 2005 IEEE International Conference on*, pp. 2161–2166, IEEE, 2005.

[14] D. Wang and M. Pham, "Unified control design for autonomous car-like vehicle tracking maneuvers," *Autonomous Mobile Robots: Sensing, Control, Decision-Making and Applications*, 2006.

[15] L. Consolini, F. Morbidi, D. Prattichizzo, and M. Tosques, "Leader–follower formation control of nonholonomic mobile robots with input constraints," *Automatica*, vol. 44, no. 5, pp. 1343–1349, 2008.

[16] R. E. Caicedo, J. Valasek, and J. L. Junkins, "Preliminary results of one-dimensional vehicle formation control using a structural analogy," in *American Control Conference, 2003. Proceedings of the 2003*, vol. 6, pp. 4687–4692, IEEE, 2003.

[17] W. Dong and Y. Guo, "Formation control of nonholonomic mobile robots using graph theoretical methods," *Cooperative Systems*, pp. 369–386, 2007.

[18] H. H. González-Banos, D. Hsu, and J.-C. Latombe, "Motion planning: Recent developments," *Autonomous Mobile Robots: Sensing, Control, Decision-Making and Applications*, 2006.

[19] S. R. Lindemann and S. M. LaValle, "Current issues in sampling-based motion planning," *Robotics Research*, pp. 36–54, 2005.

[20] J. T. Schwartz and M. Sharir, "A survey of motion planning and related geometric algorithms," *Artificial Intelligence*, vol. 37, no. 1-3, pp. 157–169, 1988.

[21] K. Komoriya and K. Tanie, "Trajectory design and control of a wheel-type mobile robot using b-spline curve," in *Intelligent Robots and Systems' 89. The Autonomous Mobile Robots and Its Applications. IROS'89. Proceedings., IEEE/RSJ International Workshop on*, pp. 398–405, IEEE, 1989.

[22] G. Vazquez, J. H. Sossa-Azuela, S. Díaz-de León, L. Juan, *et al.*, "Auto guided vehicle control using expanded time b-splines," in *Proceedings of the 1994 IEEE International Conference on Systems, Man and Cybernetics. Part 1 (of 3)*, 1994.

[23] H. Eren, C. C. Fung, and J. Evans, "Implementation of the spline method for mobile robot path control," in *Instrumentation and Measurement Technology Conference, 1999. IMTC/99. Proceedings of the 16th IEEE*, vol. 2, pp. 739–744, IEEE, 1999.

[24] M. Khatib, H. Jaouni, R. Chatila, and J.-P. Laumond, "Dynamic path modification for car-like nonholonomic mobile robots," in *Robotics and Automation, 1997. Proceedings., 1997 IEEE International Conference on*, vol. 4, pp. 2920–2925, IEEE, 1997.

[25] J.-H. Hwang, R. C. Arkin, and D.-S. Kwon, "Mobile robots at your fingertip: Bezier curve on-line trajectory generation for supervisory control," in *Intelligent Robots and Systems, 2003.(IROS 2003). Proceedings. 2003 IEEE/RSJ International Conference on*, vol. 2, pp. 1444–1449, IEEE, 2003.

[26] A. Piazzi, C. L. Bianco, M. Bertozzi, A. Fascioli, and A. Broggi, "Quintic g^2 -splines for the iterative steering of vision-based autonomous vehicles," *IEEE Transactions on Intelligent Transportation Systems*, vol. 3, no. 1, pp. 27–36, 2002.

[27] Z. Qu, J. Wang, and C. E. Plaisted, "A new analytical solution to mobile robot trajectory generation in the presence of moving obstacles," *IEEE transactions on robotics*, vol. 20, no. 6, pp. 978–993, 2004.

[28] S. Dominguez, A. Ali, G. Garcia, and P. Martinet, "Comparison of lateral controllers for autonomous vehicle: Experimental results," in *Intelligent Transportation Systems (ITSC), 2016 IEEE 19th International Conference on*, pp. 1418–1423, IEEE, 2016.

[29] A. Ali, *Modeling and control of a platoon of urban autonomous vehicles.* PhD thesis, : Institut de Recherche en Communication s et Cybernétique de Nantes (IRCCyN), 2015.

[30] P. Martinet, "Lecture notes in autonomous vehicles."